

Supporting Information:

Implications for an imidazol-2-yl carbene intermediate in the rhodanase-catalyzed C-S bond formation reaction of anaerobic ergothioneine biosynthesis

Ronghai Cheng,^{†1} Rui Lai,^{†1} Chao Peng,^{†2} Juan Lopez,¹ Zhihong Li,² Nathchar Naowarojna,¹ Kelin Li,¹ Christina Wong,¹ Norman Lee,¹ Stephen A. Whelan,¹ Lu Qiao,¹ Mark W. Grinstaff,^{1,3} Jiangyun Wang,⁴ Qiang Cui,^{1*} and Pinghua Liu^{1*}

¹Department of Chemistry, Boston University, Boston, Massachusetts 02215, United States;

²National Facility for Protein Science in Shanghai, Zhangjiang Lab, Shanghai Advanced Research Institute, Chinese Academy of Science, Shanghai 201210, China;

³Department of Biomedical Engineering, Boston University, Boston, MA 02215, USA;

⁴Institute of Biophysics, Chinese Academy of Sciences, Beijing 100101, People's Republic of China

*Email: Pinghua Liu: pinghua@bu.edu; Qiang Cui: qiangcui@bu.edu

Index

Materials and methods.	4
Additional Discussions	6
Supporting Tables	8
Supporting figures	9
Figure S1. SDS-PAGE analysis of MetC purification.....	9
Figure S2. Mass spectrometry analysis of cysteine polysulfide species from EanB-MetC coupled reaction.....	10
Figure S3. ¹ H-NMR analysis of EanB-MetC coupled reaction.....	11
Figure S4. ¹ H-NMR analysis of non-enzymatic hercynine deuterium exchange reaction at different temperatures.	12
Figure S5. Hercynine deuterium exchange experiment using EanB in the absence of MetC and selenocystine.	13
Figure S6. The extracted ion chromatograph of [ε-D]-hercynine and [ε-H] hercynine in the EanB MetC coupled deuterium exchange experiments	14
Figure S7. MS spectrometry analysis of EanB catalyzed deuterium exchanged experiment with MetC and selenocystine as the selenium source.	15
Figure S8. MS/MS spectrum of tryptic peptides from EanB-MetC coupled reaction using selenocystine as substrate, confirming the production of EanB Cys116 perselenide modification.....	16
Figure S9. MS/MS spectrum of tryptic peptides from EanB-MetC coupled reaction using selenocystine as substrate confirming EanB Cys184 perselenide modification.	16
Figure S10. MS/MS spectrum of tryptic peptides from EanB-MetC coupled reaction using selenocystine as substrate confirming EanB Cys339 perselenide modification.	17
Figure S11. MS/MS spectrum of tryptic peptides from EanB-MetC coupled reaction using selenocystine as substrate confirming EanB Cys370 perselenide modification.	17
Figure S12 ¹ H-NMR analysis of hercynine deuterium exchange in EanB _{C412-only} -MetC coupled reaction using selenocystine as the substrate.	18
Figure S13. The extracted ion chromatograph of [ε-D]-hercynine and [ε-H] hercynine in the EanB _{C412-only} MetC coupled deuterium experiments	19
Figure S14. MS spectrometry analysis of EanB _{C412-only} -MetC coupled reaction.	20
Figure S15. Hercynine deuterium exchange experiment in EanB _{C412S} -MetC coupled reaction using selenocystine as the substrate.....	21
Figure S16 Characterization of 3,5-difluoro tyrosine.....	22
Figure S17. SDS-PAGE analysis of EanB _{Y353F2Tyr} purification.....	23
Figure S18. Hercynine concentration dependence of EanB _{Y353F2Tyr} mutant using K ₂ S _x as substrate.....	24
Figure S19 ¹ H-NMR analysis of hercynine deuterium exchange experiment in EanB _{Y353F2Tyr} -MetC coupled reaction using selenocystine as substrate.	25
Figure S20. The extracted ion chromatograph of [ε-D]-hercynine and [ε-H] hercynine in the EanB _{Y353F2Tyr} MetC coupled deuterium experiments.	26
Figure S21. Deuterium exchange experiment using EanB _{WT} with equimolar hercynine and ergothioneine.	27
Figure S22. Hercynine deuterium exchange experiment in EanB _{Y353A} -MetC coupled reaction using selenocystine as substrate.	28
Figure S23. The QM cluster model used in the calculation.	29
Figure S24. The reaction of persulfide with imidazole.....	29
Figure S25. Proposed catalytic mechanisms for EanB with neutral persulfide.	30
Figure S26. Possible intermediates with neutral persulfide.	30
Figure S27. The possible proton transfer reactions involved in the EanB catalysis.	31
Figure S28. The possible pathways for the final step of EanB with neutral persulfide.....	31

Figure S29. The potential energy surface at DFTB3/3OB level of theory for the formation of C-S bond through either a tetrahedral intermediate or carbene intermediate.	32
Figure S30. The potential energy surface for the product formation involving the carbene intermediate of persulfide (A) and neutral persulfide (B) at DFTB3/3OB level of theory.	33
Reference.....	33

Materials and methods.

Selenocystine was purchased from Sigma-Aldrich. Hercynine was synthesized from previously published protocol.¹ Proton nuclear magnetic resonance spectra were recorded using Agilent 500 (500 MHz VNMRS). Reaction products were analyzed by LC-MS on a LTQ-FT-ICR mass spectrometer (Thermo Scientific). Hercynine concentration was quantified using on an Agilent 1290 UPLC (Agilent, USA) coupled to an AB Sciex 6500 QTRAP mass spectrometer (AB Sciex, USA) with the electrospray ionization (ESI) source. Peptide MS/MS analysis was performed by a Q-Exactive mass spectrometer.

Protein overexpression and purification.

The EanB and its variants was prepared as previously described protocol.² MetC gene (accession number NP_417481) was amplified from *E. coli* with forward primer 5'-GTCGCGGATCCGAATTCGCGGACAAAAGCTT-3' and reverse primer 5'-GGTGGTGGTGCCTCGAGTACAATTCGCGCAA -3' (The BamHI and XhoI digestion are indicated with underline). The sequence was sub-cloned into pET28a-(+) vector and BL21(DE3) was transformed with the recombinant plasmid. MetC protein was overexpressed following procedure of EanB, however, instead of D-glucose and potassium phosphate (KPi) buffer, PLP was added to 0.1 mM final concentration. Then, cells were incubated at 16 °C for 8 hr before harvest by centrifugation. The coding sequence of tyrosine phenol lyase (TPL) from *Citrobacter freundii* was synthesized to pET28a-(+) vector and the condon-optimized by Genescript. The protein overexpression condition is similar to MetC protein overexpression condition, except that the cells were incubated at 25 °C for 12 hours after IPTG induction.

The following procedures of MetC purification were carried out under anaerobic environment. 10 g cells were resuspended in 50 ml lysis buffer (100 mM Tris-HCl, 300 mM NaCl, pH 8.0) with 1 mg/mL final concentration of lysozyme. The mixture was incubated on ice with shaking for 30 min. Cells were lysed by sonication (505 Sonic Dismembrator). PLP was added to cell lysate to 0.1 mM final concentration. Cell debris was removed via centrifugation at 20,000 rpm for 30 min, 4 °C. The supernatant was incubated with 5 mL of Ni Sepharose resin (GE Healthcare). The column was washed with 25 mL of lysis buffer with 30 mM imidazole and 0.1 mM PLP followed by 25 mL lysis buffer with 30 mM imidazole. The protein was eluted by lysis buffer containing 250 mM imidazole and concentrated using ultrafiltration (Millipore). The imidazole was removed from concentrated protein using a G25 Sephadex size-exclusion column (30×600 mm). The fractions containing MetC protein were pooled and concentrated through ultrafiltration. The exact active protein concentration was corrected by PLP content quantification using published protocol.³

The purification process of TPL was similar to CBL protein except that the purification process was done aerobically.

Characterizations of EanB-MetC coupled reaction using cystine as sulfur source.

The reaction was characterized by ¹H-NMR analysis, UV-vis kinetics analysis and mass spectrometry analysis.

¹H-NMR analysis.

A 1-mL reaction contained 2 μM EanB, 1 mM hercynine, 1 mM cystine, and 4 nM MetC in 10 mM Tris-HCl, pH 8.0 at room temperature for 8 hr. The reaction was lyophilized, dissolved in 300 μL D₂O and ergothioneine formation was determined using ¹H-NMR assay.

For selenoneine detection reaction, a 1-mL reaction contained 50 μM EanB, 3 mM hercynine, selenocystine saturated solution (containing 3.4mg powder), and 0.5 μM MetC in 50 mM KPi buffer, pH 8.0 at room temperature for 8 hr. The reaction was lyophilized, dissolved in 300 μL D₂O and selenoneine formation was determined using ¹H-NMR assay.

UV-vis kinetics analysis.

1 ml reaction mixture was composed of 2-10 μM EanB, 4 nM MetC, 1 mM Cystine, 1 mM hercynine in 10 mM Tris-HCl, pH = 8.0 buffer. Ergothioneine from Burkholderia sp. HME13 was added to a final concentration of 400 nM. The rate of thio-urocanic acid ($\epsilon_{311\text{nm}} = 1.8 \times 10^5 \text{ M}^{-1}\cdot\text{cm}^{-1}$) formation was monitored at 311 nm for 30 min.

Mass spectrometry analysis.

Under anaerobic condition, a 5-ml reaction containing 2 μ M EanB, 4 nM MetC, 1 mM hercynine, and 1 mM cystine in 10 mM Tris-HCl, pH 8.0 was set up at room temperature. After 5 min and 30 min, 2-mL aliquot of the reaction was quenched with addition of 1 mL chloroform. The mixture was vortex for 3 minutes. The precipitated protein was removed by centrifugation at 15,000 rpm. Then, cysteine polysulfide was alkylated with iodoacetamide to 1 mM final concentration under the dark conditions for 1 hr at room temperature. The samples were then subjected to LC/MS (linear gradient from 5% to 90% MeOH with 0.1% formic acid for 30 minutes, 0.5 mL \cdot min⁻¹ and 20 μ L sample was analyzed using C18 column (YMC-triart). The reaction was repeated in two independent trials.

Synthesis of 3,5-difluorotyrosine

The synthesis method of 3,5-difluorotyrosine referred to the following established methods.⁴ Typically, 1 liter of enzymatic reaction mixture with 10 mM 2,6-difluorophenol, 30 mM ammonium acetate, 60 mM sodium pyruvate, 5 mM β -mercaptoethanol, 40 μ M PLP, 50 mM KPi buffer (pH=8.0) and 40 mg of purified TPL protein was setup. The reaction was incubated in the dark with stirring at 25 $^{\circ}$ C for 4 days. The reaction mixture was acidified to pH=3.0 with 6 M HCl and the precipitated protein was removed by celite filtration. The filtrate was extracted by 500 mL of ethyl acetate. The aqueous layer was loaded onto a 100 mL Dowex 50WX8-100 cation exchange column (from Sigma-Aldrich). The column was washed by 500 mL of 30% ACN in H₂O. The 3,5-difluorotyrosine acid was then eluted by 6 % ammonium hydroxide water solution. Fractions with product were combined and lyophilized.

Additional Discussions

Reactivity of Neutral Persulfide. We employed small molecule models at CPCM/B3LYP-D3/6-31+G(d,p) level of theory to understand the reactivity of persulfide in its neutral form (i.e. Cys-S-S-H). The electronic energy difference (ΔE) between the reactant and product for negatively charged persulfide and neutral persulfide are examined, as shown in Figure S24. The ΔE for persulfide and neutral persulfide are -3.4 kcal/mol and -12.5 kcal/mol, respectively, suggesting that the neutral persulfide is energetically feasible in EanB-catalysis. The proposed catalytic mechanism for EanB with neutral persulfide is shown in Figure S25.

First, in EanB, the reaction has to be initiated with the imidazole ring protonation, so both persulfide and neutral form persulfide shares the same first step with Tyr353 donating the proton to mercynine N atom. The next step may involve a tetrahedral intermediate or a carbene intermediate, as we discussed in our previous paper.²

Four possible tetrahedral or pyramidal intermediates have been examined, as shown in Figure S26. The first tetrahedral intermediate has a proton on persulfide, as shown in Figure S26A. This tetrahedral intermediate is not stable, suggesting that, to form a stable tetrahedral intermediate, the neutral persulfide has to donate its proton to a base, i.e. deprotonated Tyr353 in EanB. The second and third ones are pyramidal intermediates (with no H atom on the C atom, as shown in Figure S26B and S26C). These intermediates are not stable, indicating that there are no intermediates between carbene intermediate and the final product. The only stable tetrahedral intermediate is the structure shown in Figure S26D. Therefore, for neutral persulfide, the deprotonated tyrosine has to act as a base to accept the proton on the persulfide to form the tetrahedral intermediate (Figure S26D). The reaction for the formation of tetrahedral intermediate is shown in Figure S26E. The electronic energy difference (ΔE) between the left side (protonated imidazole intermediate) and right side (tetrahedral intermediate) is -9.1 kcal/mol, indicating that the reaction is energetically favorable, if the deprotonated tyrosine acts as a proton acceptor for the neutral persulfide.

Now the question becomes whether a deprotonated tyrosine would like to take a proton from neutral persulfide to form a tetrahedral intermediate (Path I in Figure S25) or from the C-H of imidazole ring to form a carbene intermediate (Path II in Figure S25). We examined the proton transfer step by using small molecule models at CPCM/B3LYP-D3/6-31+G(d,p) level of theory, as shown in Figure S27. The ΔE for the formation of carbene intermediate by deprotonated tyrosine is -23.5 kcal/mol, while the ΔE for deprotonated tyrosine getting a proton from neutral persulfide is -14.4 kcal/mol. The results suggest that both reactions are energetically feasible, though deprotonated tyrosine prefers getting a proton from the C-H of imidazole ring to ensure a better stability.

The final step is the formation of C-S bond, as shown in Figure S25 and Figure S28. This step can involve a tetrahedral intermediate, as it has a slightly lower energy as compared to that of carbene intermediate. However, this path (Path I in Figure S25) involves a proton transfer from C-H to the cystine sulfur atom, which likely encounter some difficulties, since the distance and angle are not optimal for proton transfer reactions. Another possible pathway is the electrophilic addition of sulfur atom to the C atom of the carbene intermediate by the neutral persulfide, as shown in Figure S25 Path II. The proton on persulfide can be easily transferred to the cystine during reaction. This step involves an electronic energy change (ΔE) of -37.4 kcal/mol, suggesting the reaction is energetically favorable. To further examine the reactivity of tetrahedral intermediate and carbene intermediate with neutral persulfide, we explored the potential energy surface at DFTB3/3OB level of theory, as shown in Figure S29. The direct conversion of tetrahedral intermediate to product (Path I) has an energy barrier of about 45 kcal/mol, relative to reactant state, as shown in Figure S29. The energy barrier is higher than that of Path II (about 40 kcal/mol), where a carbene intermediate is involved. The results suggest that tetrahedral intermediate is unlikely favorable in EanB catalyzed reaction.

The potential energy surfaces are also compared for persulfide and neutral persulfide at DFTB3/3OB level of theory, as shown in Figure S30. The transition state structures for persulfide and neutral persulfide are rather similar in C-S and S-S distances, though for neutral persulfide, the TS is “synchronous”: C-S bond formation and proton transfer from one sulfur to the other occurs at the same time. The electronic energy barrier is about 40 kcal/mol, relative to the reactant state, as shown in Figure S30B. For persulfide, the electronic energy barrier is about 35 kcal/mol, slightly lower than that of neutral persulfide, as shown in Figure S30A. These energy barriers are higher than those in enzyme reactions, as the transition state is likely better stabilized in EanB enzyme due to a few numbers of hydrogen bonds between persulfide and nearby residues. The higher energy barrier for neutral persulfide suggests that, in EanB enzyme reactions, the energy barrier of the rate-limiting step for neutral persulfide is also likely higher than that of persulfide.

In summary, based on the small molecule models, neutral persulfide (Cys-S-S-H) may be involved in the reaction. Nevertheless, even with neutral persulfide, our small model calculations suggest that the reaction likely involves a carbene intermediate and the reaction pathways are similar to those of negatively charged persulfide (Cys-S-S). Though the small molecule models have shed light on the reactivity of neutral persulfide (Cys-S-S-H) in EanB, further calculations by using accurate QM/MM simulation are necessary to quantitatively elucidate the protonation state of persulfide in EanB enzyme reactions and will be reported as future work.

Supporting Tables

Table S1. Relative electronic energies (ΔE , kcal/mol) and key distances (\AA) of models shown in **Fig. S22** optimized at CPCM/B3LYP-D3/6-31+G(d,p) level of theory for EanB with persulfide and perselenide.

EanB-Persulfide	ΔE	$r(\text{S}\dots\text{S})$	$r(\text{S}\dots\varepsilon\text{-C})$	$r(\varepsilon\text{-C}\dots\text{O}_{\text{Tyr}353})$	$r(\varepsilon\text{-H}\dots\varepsilon\text{-C})$	$r(\varepsilon\text{-H}\dots\text{O}_{\text{Tyr}353})$
RS	0.0	2.12	4.14	3.17	1.08	2.94
IM-1 _s	15.1	2.11	3.26	2.88	1.11	1.79
TS-1 _s	20.6	2.12	3.25	2.59	1.41	1.19
IM-3 _s	19.8	2.12	3.25	2.72	1.68	1.04
TS-2 _s	27.0	2.26	2.49	3.90	3.03	1.00
TS-3 _s	33.0	2.22	2.34	2.58	1.39	1.20
PS _s	-3.7	4.40	1.71	3.84	2.93	0.99

EanB-Perselenide	ΔE	$r(\text{S}\dots\text{Se})$	$r(\text{Se}\dots\varepsilon\text{-C})$	$r(\varepsilon\text{-C}\dots\text{O}_{\text{Tyr}353})$	$r(\varepsilon\text{-H}\dots\varepsilon\text{-C})$	$r(\varepsilon\text{-H}\dots\text{O}_{\text{Tyr}353})$
RS	0.0	2.26	3.62	3.15	1.08	2.87
IM-1 _{se}	17.1	2.24	3.34	2.85	1.11	1.75
TS-1 _{se}	21.4	2.25	3.20	2.59	1.39	1.20
IM-3 _{se}	20.0	2.27	3.06	2.75	1.72	1.03
TS-2 _{se}	22.2	2.44	2.43	3.04	2.08	0.98
PS _{se}	12.6	3.78	1.84	4.25	3.33	0.99

Supporting figures

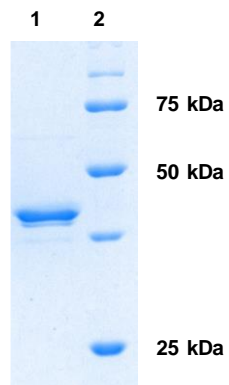


Figure S1. SDS-PAGE analysis of MetC purification.

Lane 1: purified MetC (1 μg protein was loaded); Lane 2: protein marker

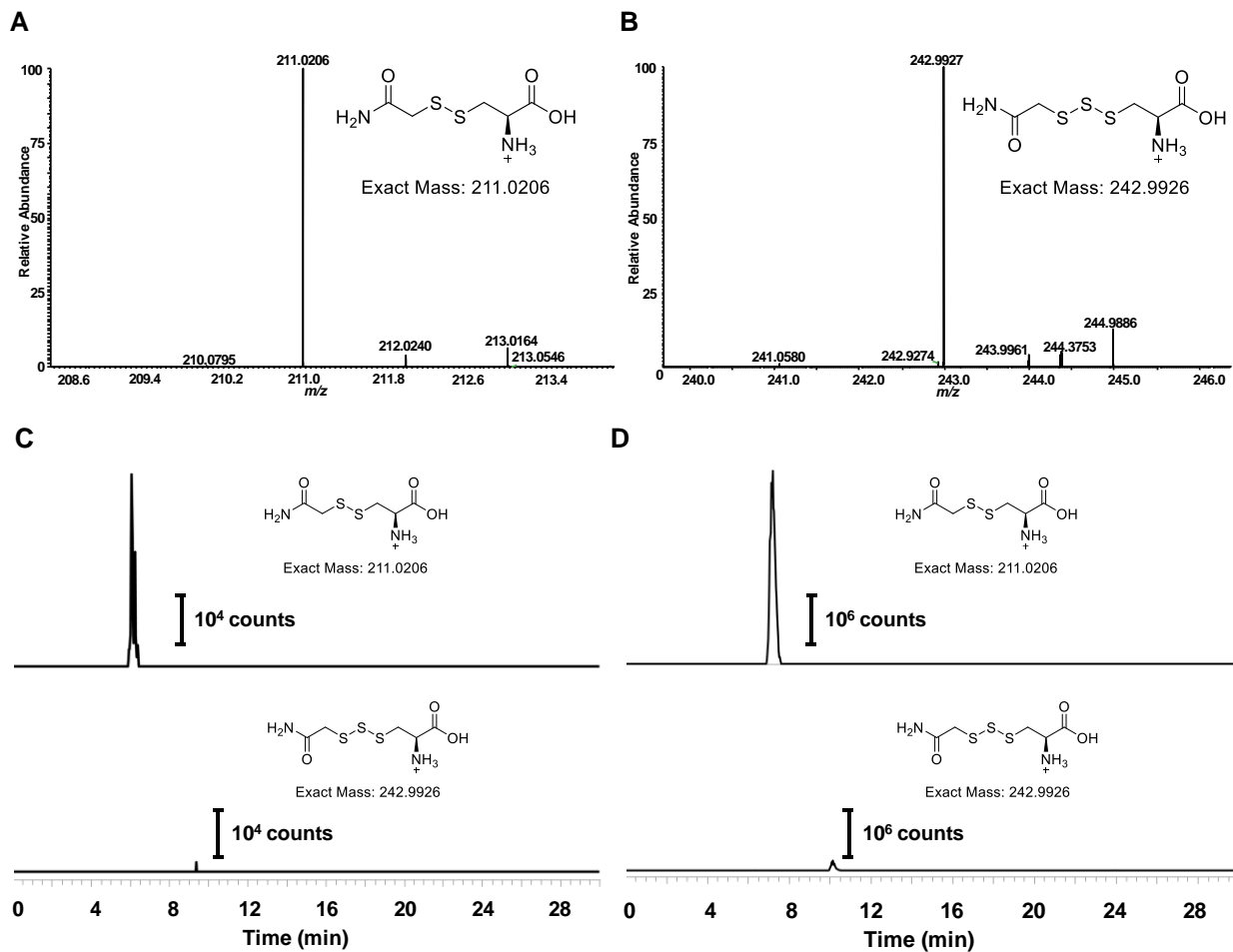


Figure S2. Mass spectrometry analysis of cysteine polysulfide species from EanB-MetC coupled reaction. (A) derivatized cysteine persulfide: calculated value for alkylated cysteine disulfide $[M+H]^+$ form (positive mode) was m/z 211.0206 and found m/z 211.0206. (B) derivatized cysteine trisulfide: Calculated value for alkylated cysteine trisulfide $[M+H]^+$ form (positive mode) was m/z 242.9926 and found m/z 242.9927. (C) Extracted ion chromatogram for cysteine polysulfide species of EanB-MetC reaction at 5 minutes. (D) Extracted ion chromatogram for cysteine polysulfide species of EanB MetC reaction at 30 minutes.

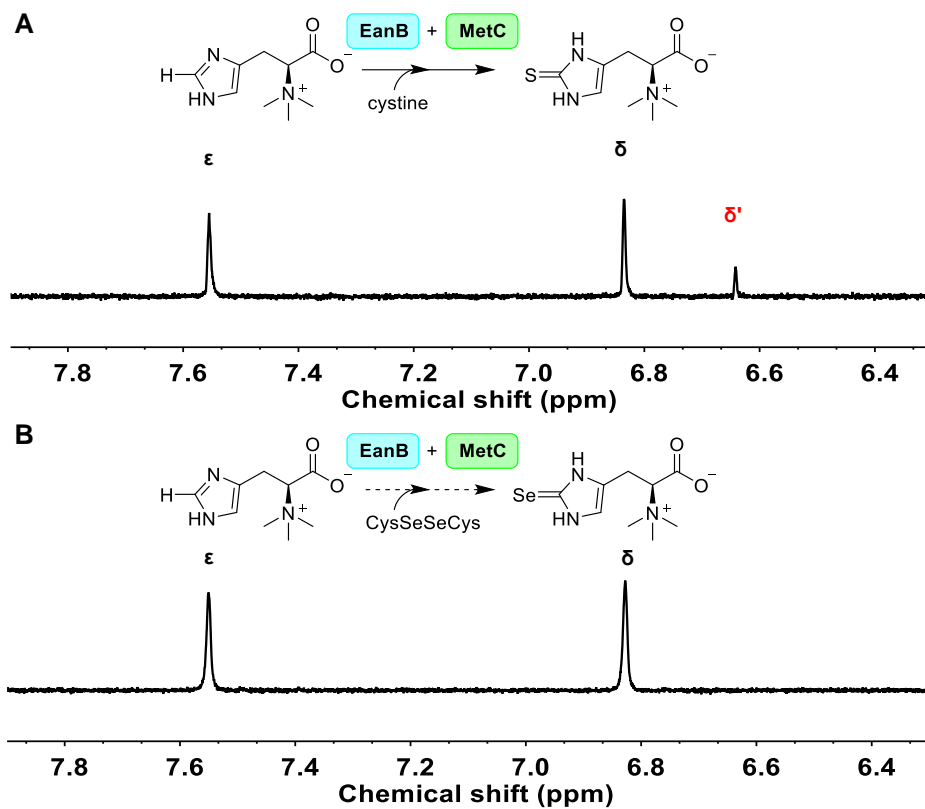


Figure S3. ¹H-NMR analysis of EanB-MetC coupled reaction.

(A) Robust ergothioneine production was observed when cystine was used as substrate. A 1-ml reaction is composed of 2 μ M EanB, 4 nM MetC, 1 mM cystine, 1 mM hercynine in 50 mM KPi buffer, pH 8.0 (B) There was no detectable selenoneine product with selenocystine as substrate. A 1-ml reaction contained 50 μ M EanB, 0.5 μ M MetC, 3 mM hercynine, saturated selenocystine solution (containing 3.4 mg powder) in 50 mM KPi buffer, pH 8.0.

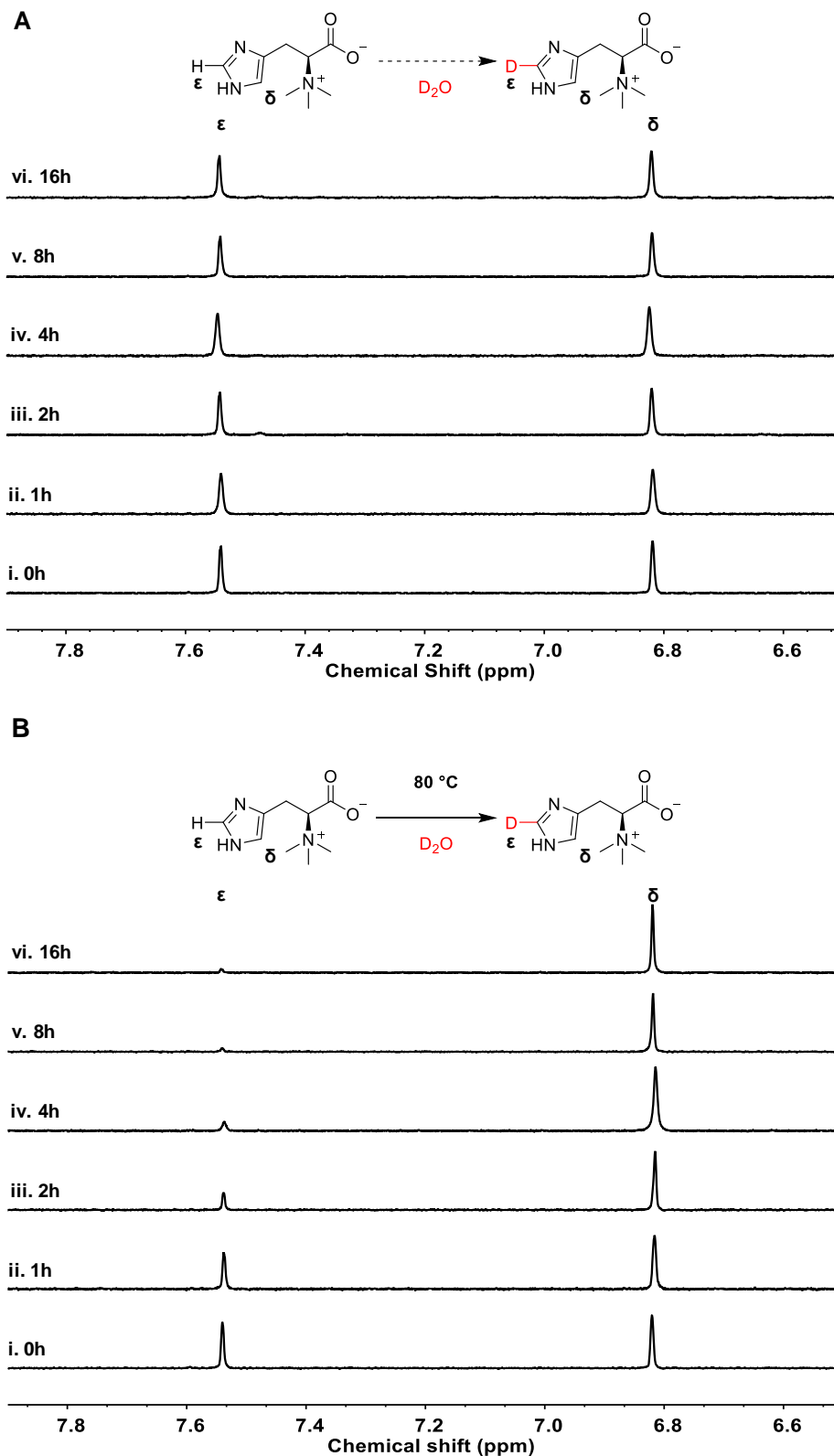


Figure S4. ^1H -NMR analysis of non-enzymatic hercynine deuterium exchange reaction at different temperatures.

(A) Reaction with 3 mM hercynine in KPi D_2O buffer, pH 8.22 at 25 °C. (B) Reaction with 3 mM hercynine in KPi D_2O buffer, pH 8.22 at 80 °C. (There was ~ 6% H_2O added so that it had the same amount of H_2O as the enzymatic reaction system)

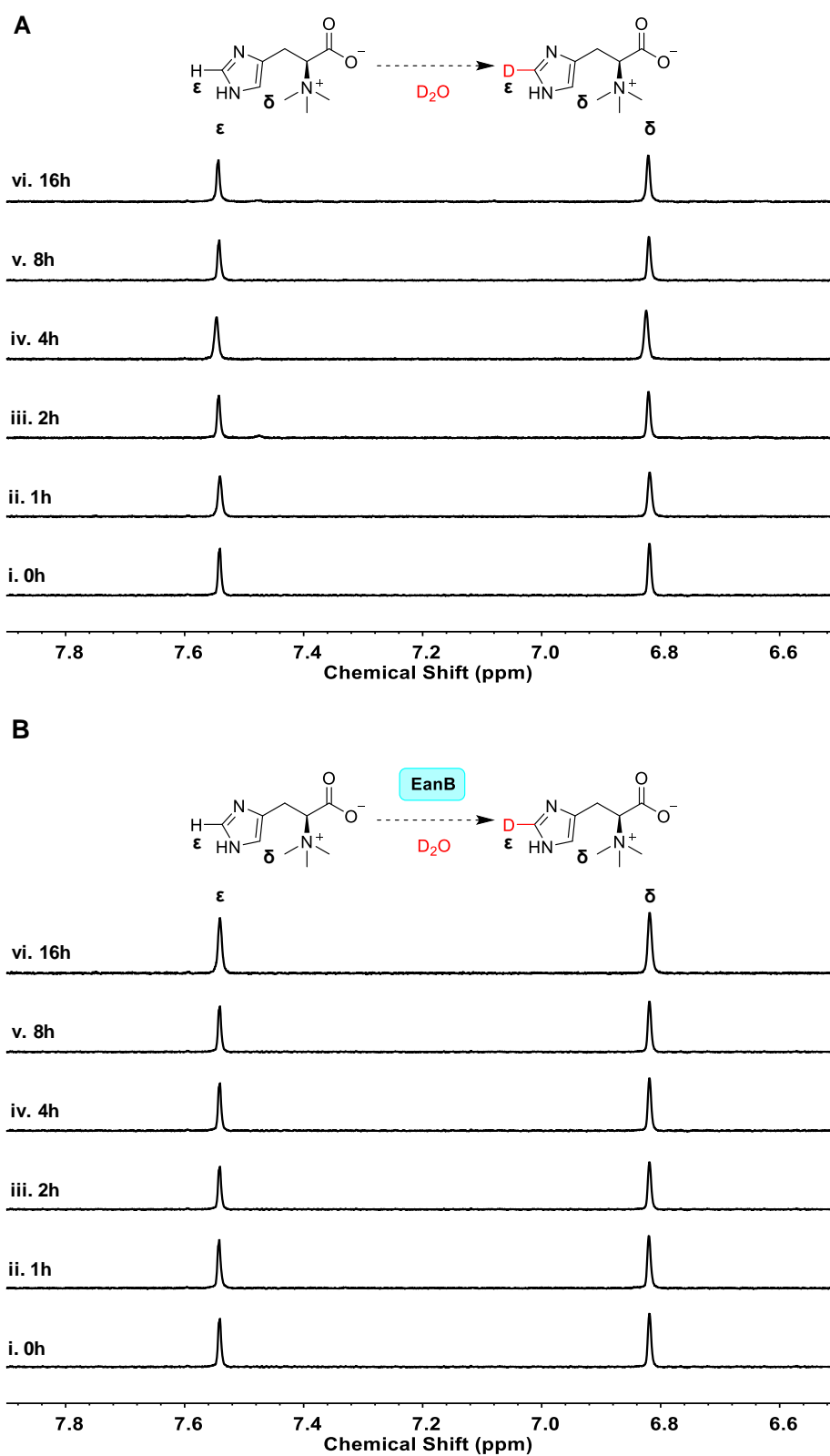


Figure S5. Hercynine deuterium exchange experiment using EanB in the absence of MetC and selenocystine. (A) Reaction with 3 mM hercynine in KPi D₂O buffer with pD of 8.22. (B) Reaction with 3 mM hercynine and 50 μ M EanB in KPi D₂O buffer with pD of 8.22.

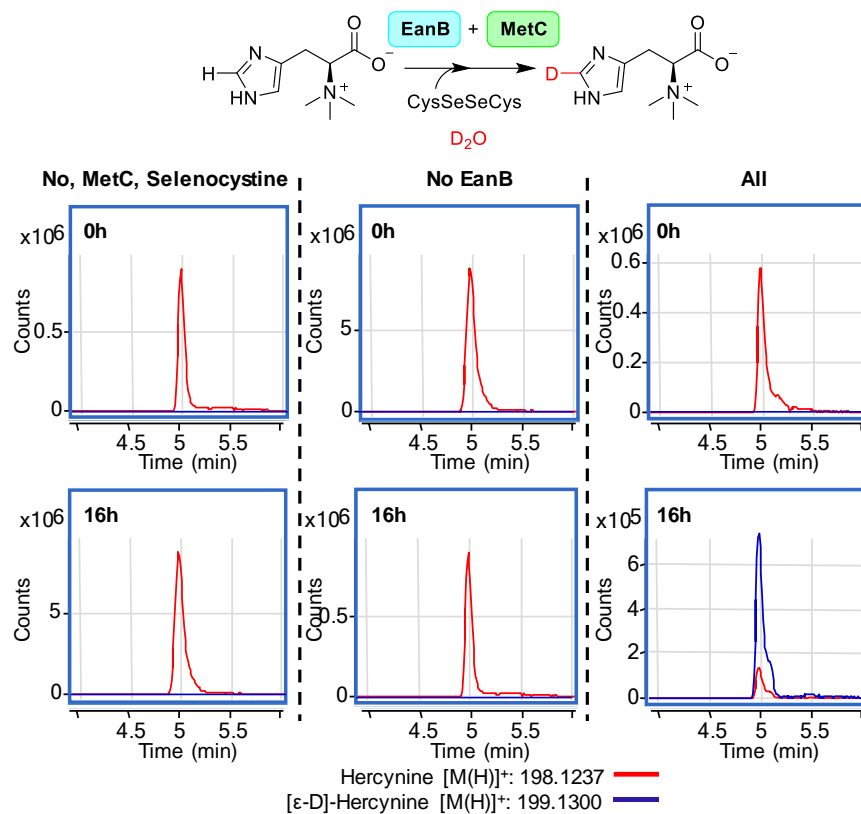


Figure S6. The extracted ion chromatograph of [ε-D]-hercynine and [ε-H] hercynine in the EanB MetC coupled deuterium exchange experiments

Aliquots of the reaction mixture at 0 hour and 16 hours were withdrawn and quantified by LC-MS analysis. The 2-ml reaction mixture contained 50 μM EanB, 0.5 μM MetC, selenocystine saturated solution (6.7 mg powder added), 3 mM hercynine in 50 mM KPi D₂O buffer with pD of 8.22. The percentage of [ε-D]-hercynine is quantified based on the peak area between [ε-D]-hercynine (m/z: 199.1300) and hercynine (m/z: 198.1237) from the extracted ion chromatograph.

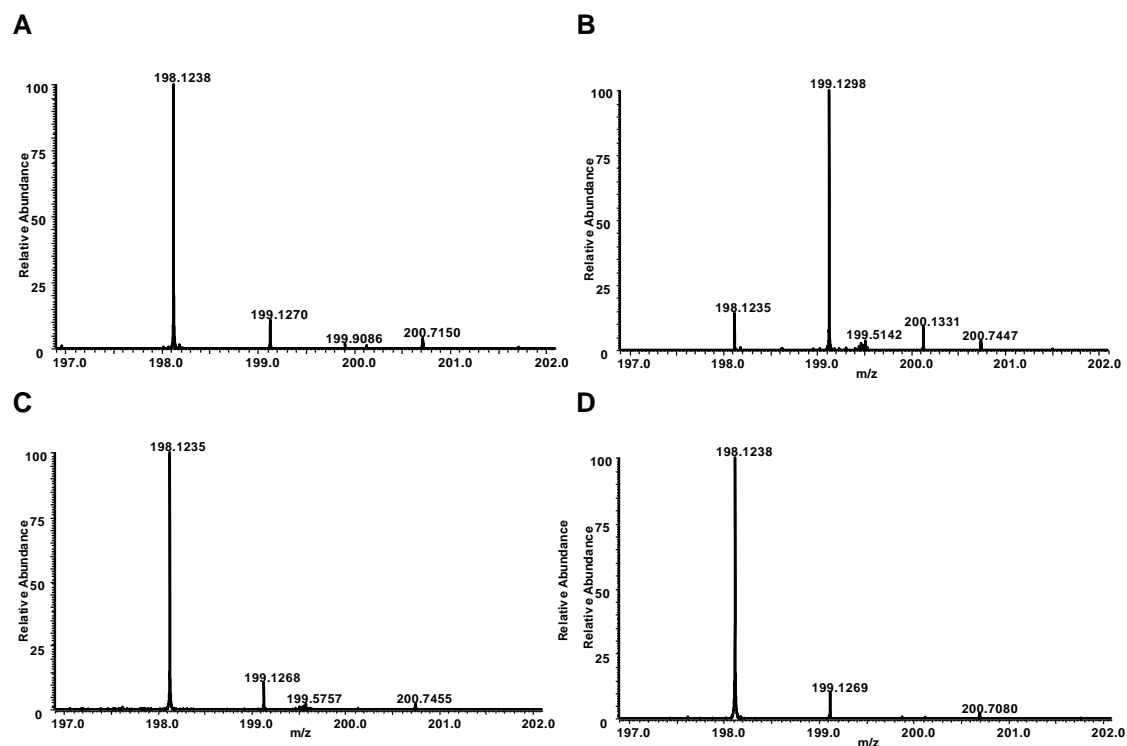


Figure S7. MS spectrometry analysis of EanB-catalyzed deuterium exchanged experiment with MetC and selenocystine as the selenium source.

Calculated value for [ϵ -D]-hercynine $[M+H]^+$ form (positive mode) was m/z 199.1300 and [ϵ -H]-hercynine $[M+H]^+$ form (positive mode) was m/z 198.1237 (A)-(B) Mass spectra of non-deuterated and deuterated hercynine from reaction mixture with EanB at (A) 0 hour and (B) 16 hours. (C)-(D) Mass spectra of non-deuterated and deuterated hercynine from reaction mixture without EanB at 0 hour (C) and 16 hours (D).

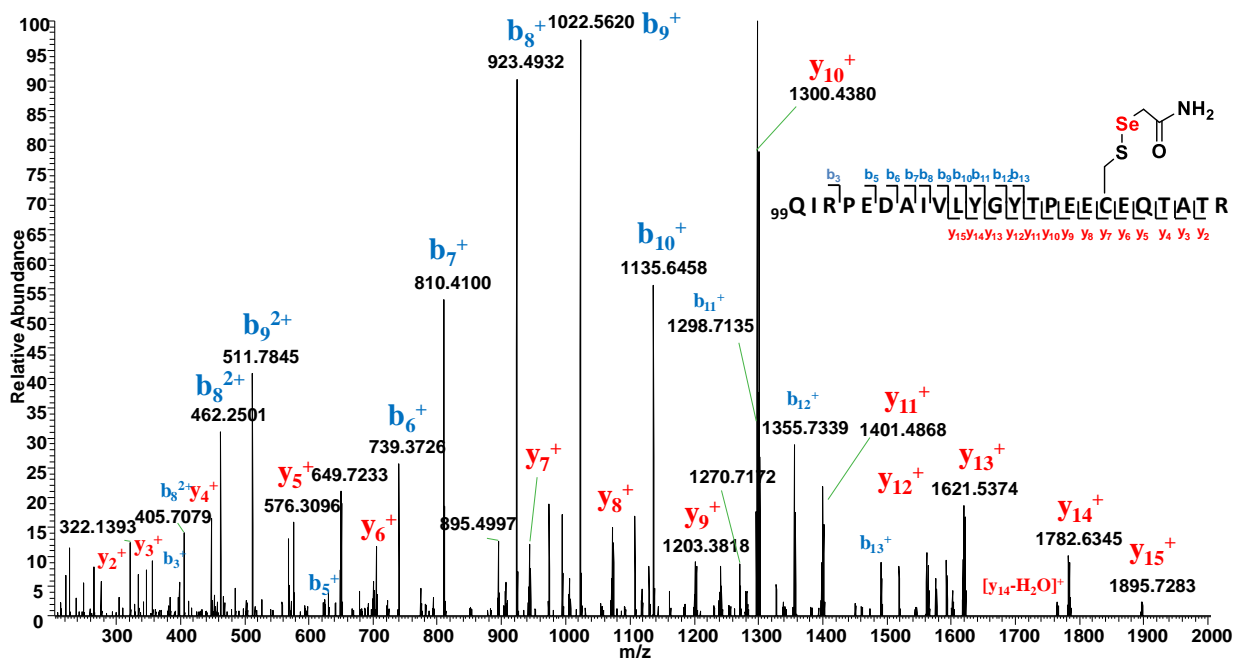


Figure S8. MS/MS spectrum of tryptic peptides from EanB-MetC coupled reaction using selenocystine as substrate, confirming the production of EanB Cys116 perselenide modification.

The Peptide fragment ion (residue 99 to residue 122) with $[M+3H]^{3+}$ at 973.7666 (predicted exact m/z: 973.7626) identified Cys116 with a Cys116-S-Se-acetamide modification, which suggested the Cys116 perselenide modification during the EanB-MetC coupled reaction.

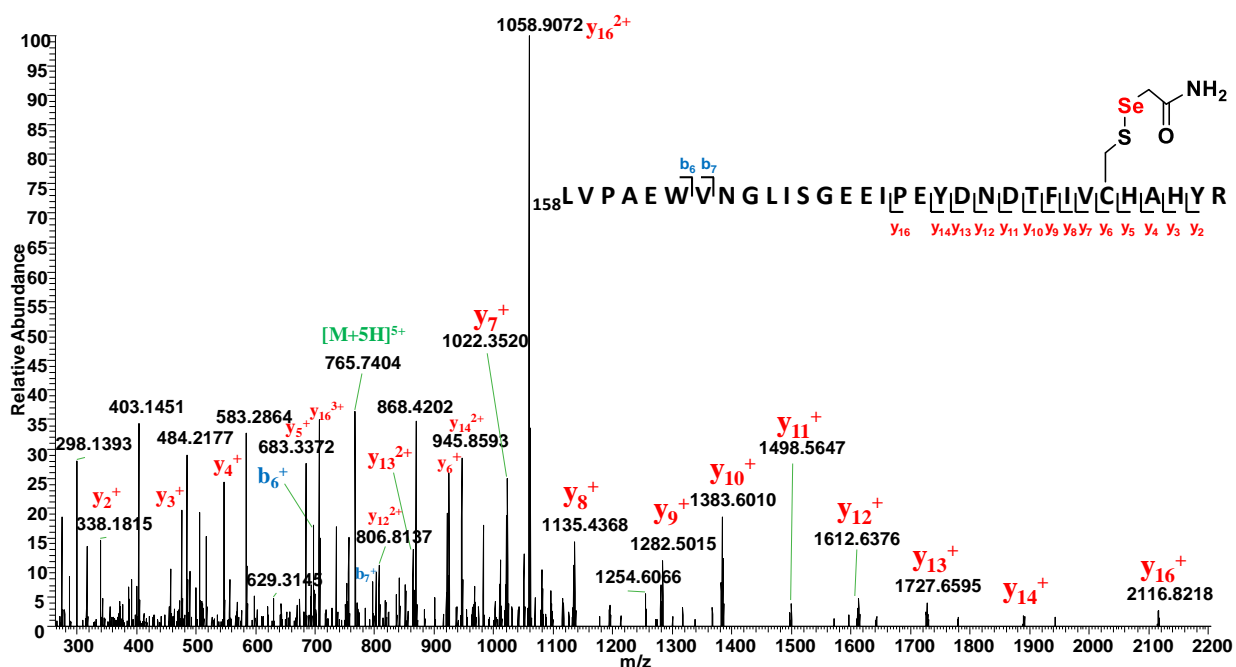


Figure S9. MS/MS spectrum of tryptic peptides from EanB-MetC coupled reaction using selenocystine as substrate confirming EanB Cys184 perselenide modification.

The Peptide fragment ion (residue 158 to residue 189) with $[M+5H]^{5+}$ at 765.5434 (predicted exact m/z: 765.5451) identified Cys184 with a Cys184-S-Se-acetamide modification, which suggested the Cys184 perselenide modification during the EanB-MetC coupled reaction.

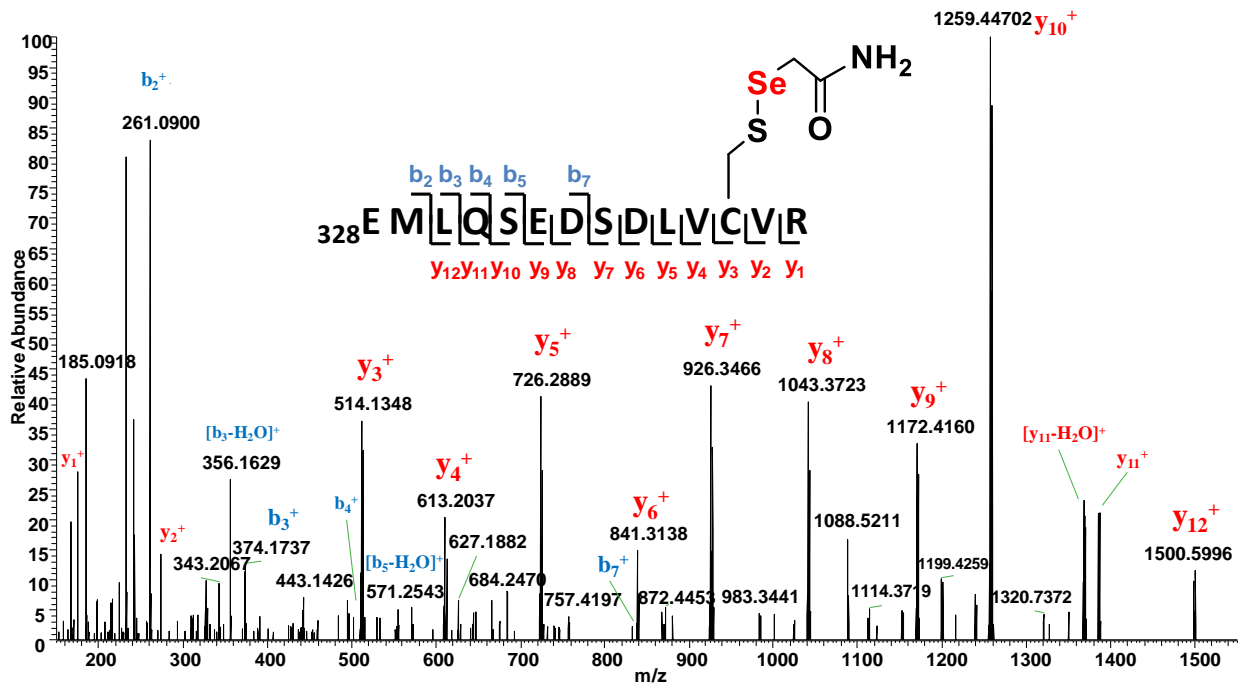


Figure S10. MS/MS spectrum of tryptic peptides from EanB-MetC coupled reaction using selenocystine as substrate confirming EanB Cys339 perselenide modification.

The Peptide fragment ion (residue 328 to residue 341) with $[M+2H]^{2+}$ at 880.8413 (predicted exact m/z : 880.8403) identified Cys339 with a Cys339-S-Se-acetamide modification, which suggested the Cys339 perselenide modification during the EanB-MetC coupled reaction.

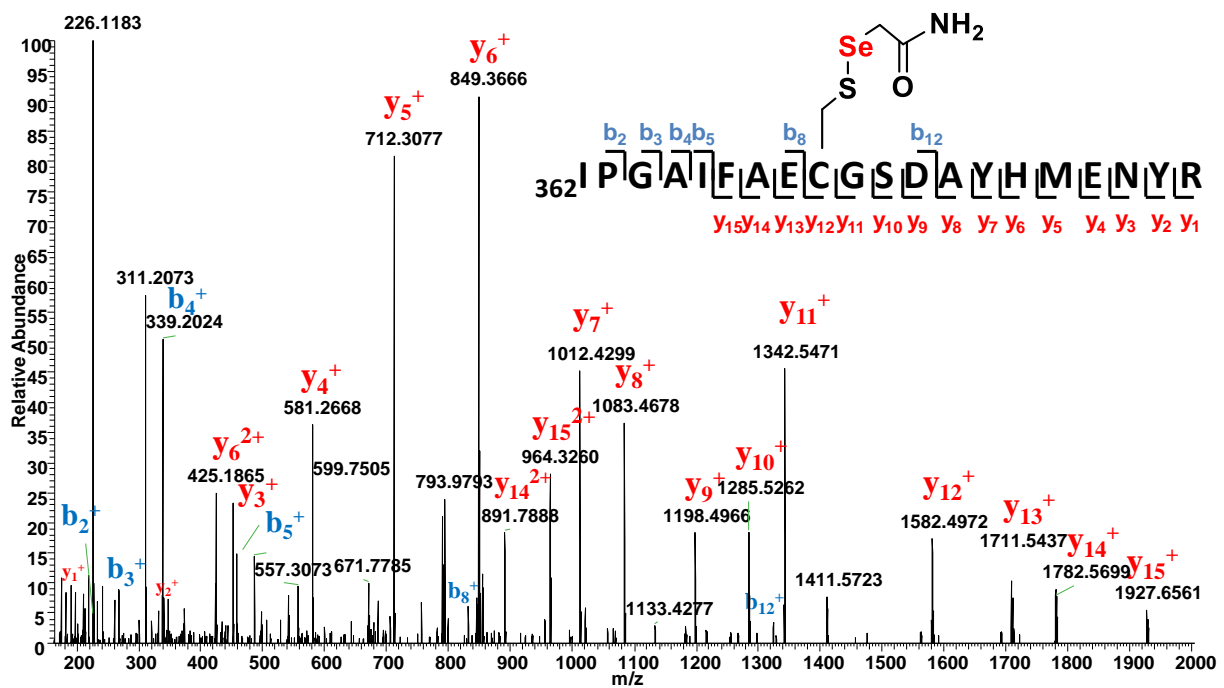


Figure S11. MS/MS spectrum of tryptic peptides from EanB-MetC coupled reaction using selenocystine as substrate confirming EanB Cys370 perselenide modification.

The Peptide fragment ion (residue 362 to residue 381) with $[M+3H]^{3+}$ at 794.3144 (predicted exact m/z : 794.3125) identified Cys370 with a Cys370-S-Se-acetamide modification, which suggested the Cys370 perselenide modification during the EanB-MetC coupled reaction.

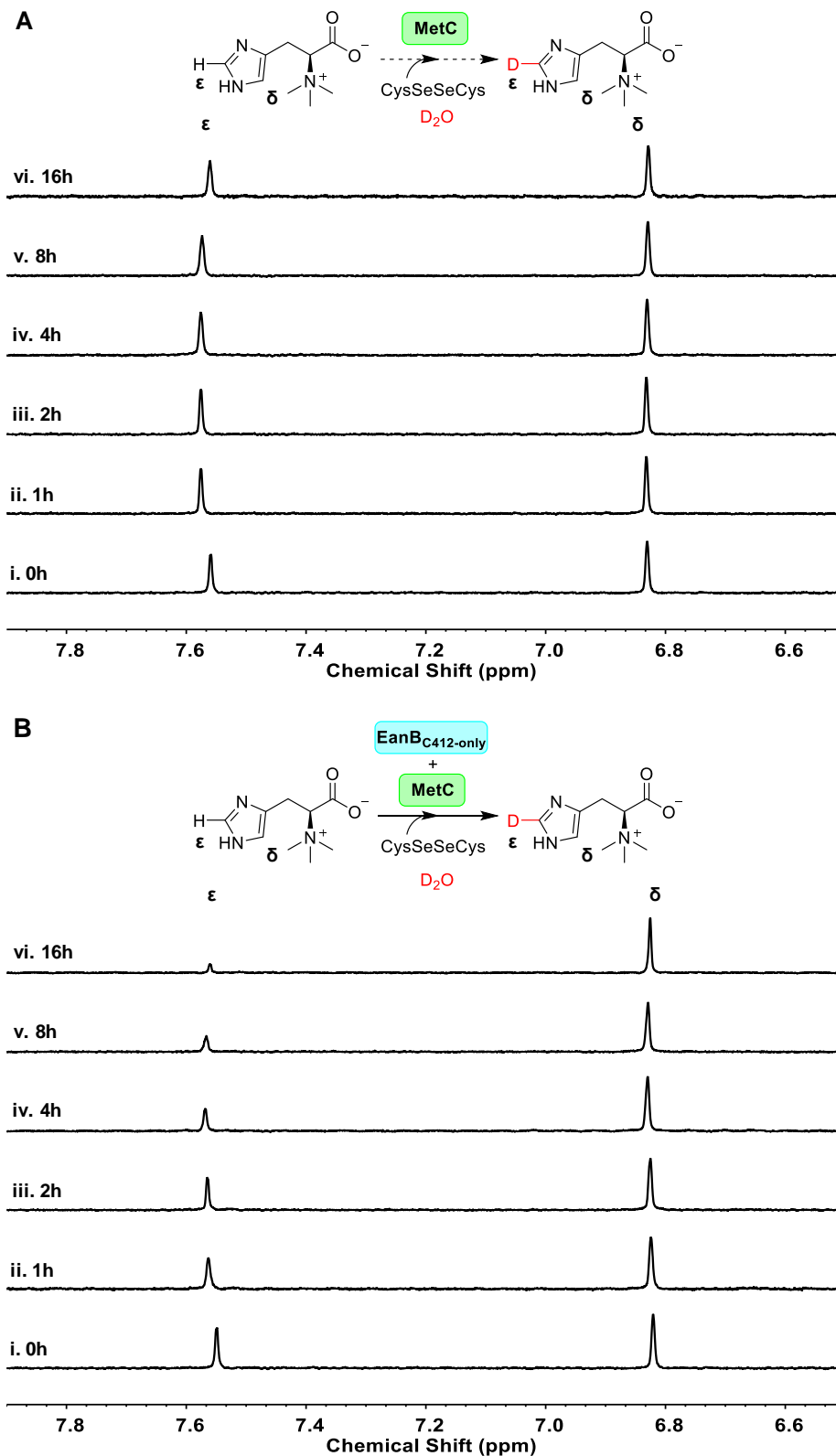


Figure S12 $^1\text{H-NMR}$ analysis of hercynine deuterium exchange in EanB_{C412-only}-MetC coupled reaction using selenocystine as the substrate.

(A) spectra from 2-ml reaction mixture with 3 mM hercynine, selenocystine saturated solution (6.7 mg powder added), 0.5 μM MetC in the absence of EanB_{C412-only} in D₂O buffer. (B) spectra from 2-ml reaction mixture with 3 mM hercynine, selenocystine saturated solution (6.7 mg powder added), 0.5 μM MetC, and 50 μM EanB_{C412-only} in D₂O buffer.

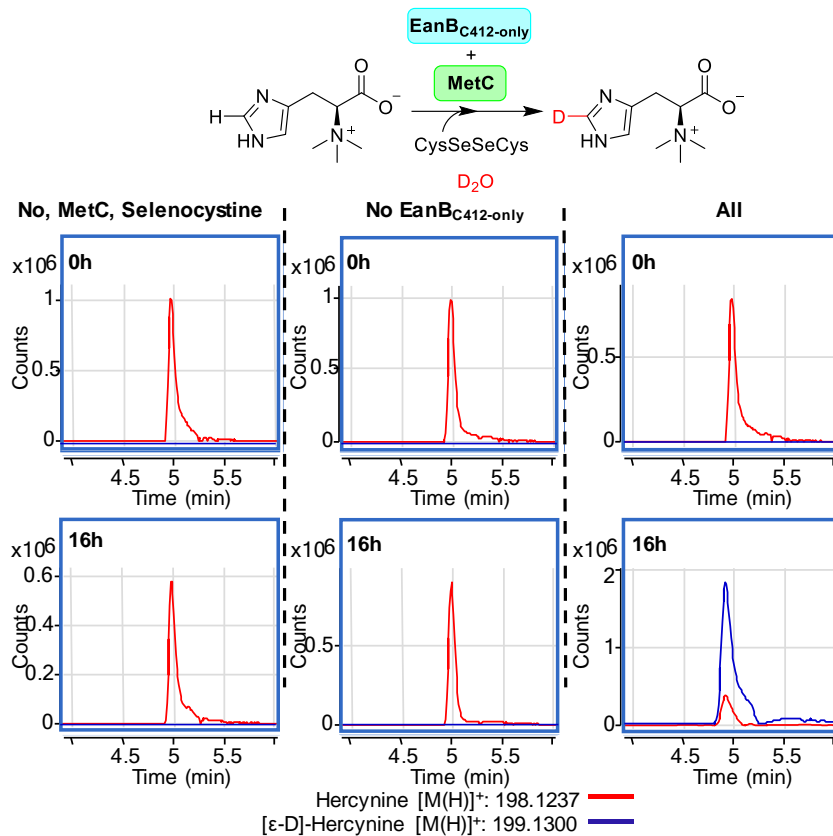


Figure S13. The extracted ion chromatograph of [ε-D]-hercynine and [ε-H] hercynine in the EanB_{C412-only} MetC coupled deuterium experiments

The reaction mixture at 0 hour and 16 hours were withdrawn and analyzed by LC-MS analysis. The 2-ml reaction mixture contained 50 μM EanB_{C412-only}, 0.5 μM MetC, selenocystine saturated solution (6.7 mg powder added), 3 mM hercynine in 50 mM KPi D₂O buffer with pD of 8.22. The percentage of [ε-D]-hercynine is quantified based on the peak area between [ε-D]-hercynine (m/z: 199.1300) and hercynine (m/z: 198.1237) from the extracted ion chromatograph.

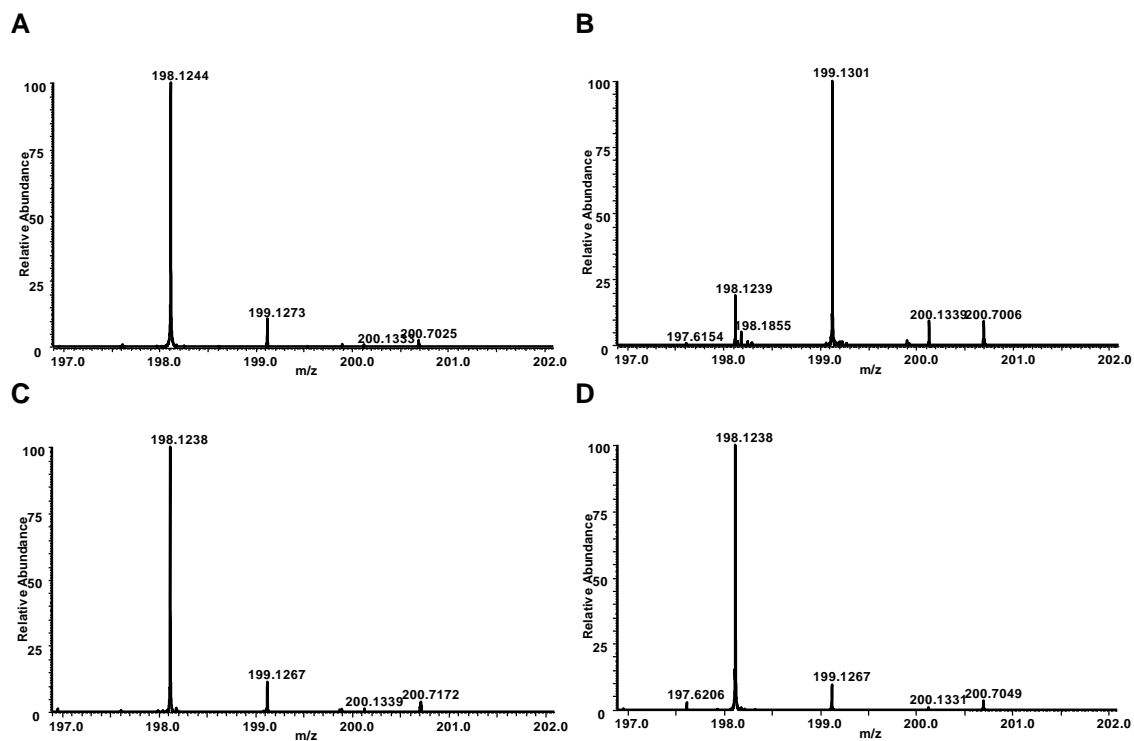


Figure S14. MS spectrometry analysis of EanB_{C412-only}-MetC coupled reaction.

Calculated value for [ϵ -D]-hercynine [M+H]⁺ form (positive mode) was m/z 199.1300 and [ϵ -H]-hercynine [M+H]⁺ form (positive mode) was m/z 198.1237 (A)-(B) Mass spectra of non-deuterated and deuterated hercynine from reaction mixture with EanB_{C412-only} at (A) 0 hour and (B) 16 hours. (C)-(D) Mass spectra of non-deuterated and deuterated hercynine from reaction mixture in the absence of EanB_{C412-only} at 0 hour (C) and 16 hours (D).

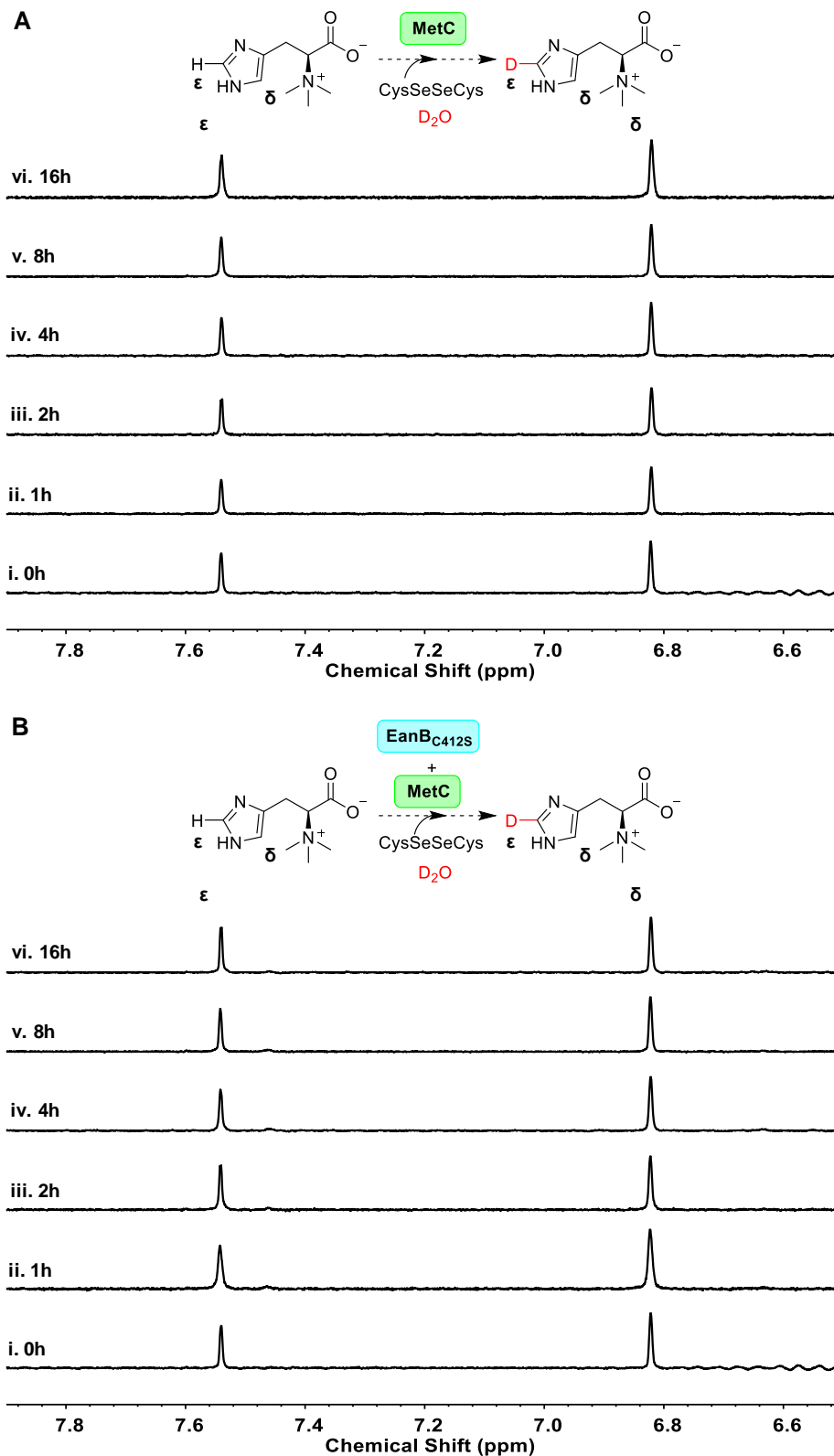


Figure S15. Hercynine deuterium exchange experiment in EanB_{C412S}-MetC coupled reaction using selenocystine as the substrate.

(A) Reaction mixture (2 ml) with 3mM hercynine, selenocystine saturated solution (6.7 mg powder added), 0.5 μ M MetC in the absence of EanB_{C412S} in 50 mM KPi D_2O buffer (B) Reaction mixture (2 ml) with 3mM hercynine, selenocystine saturated solution (6.7 mg powder added), 0.5 μ M MetC, and 50 μ M EanB_{C412S} in 50 mM KPi D_2O buffer.

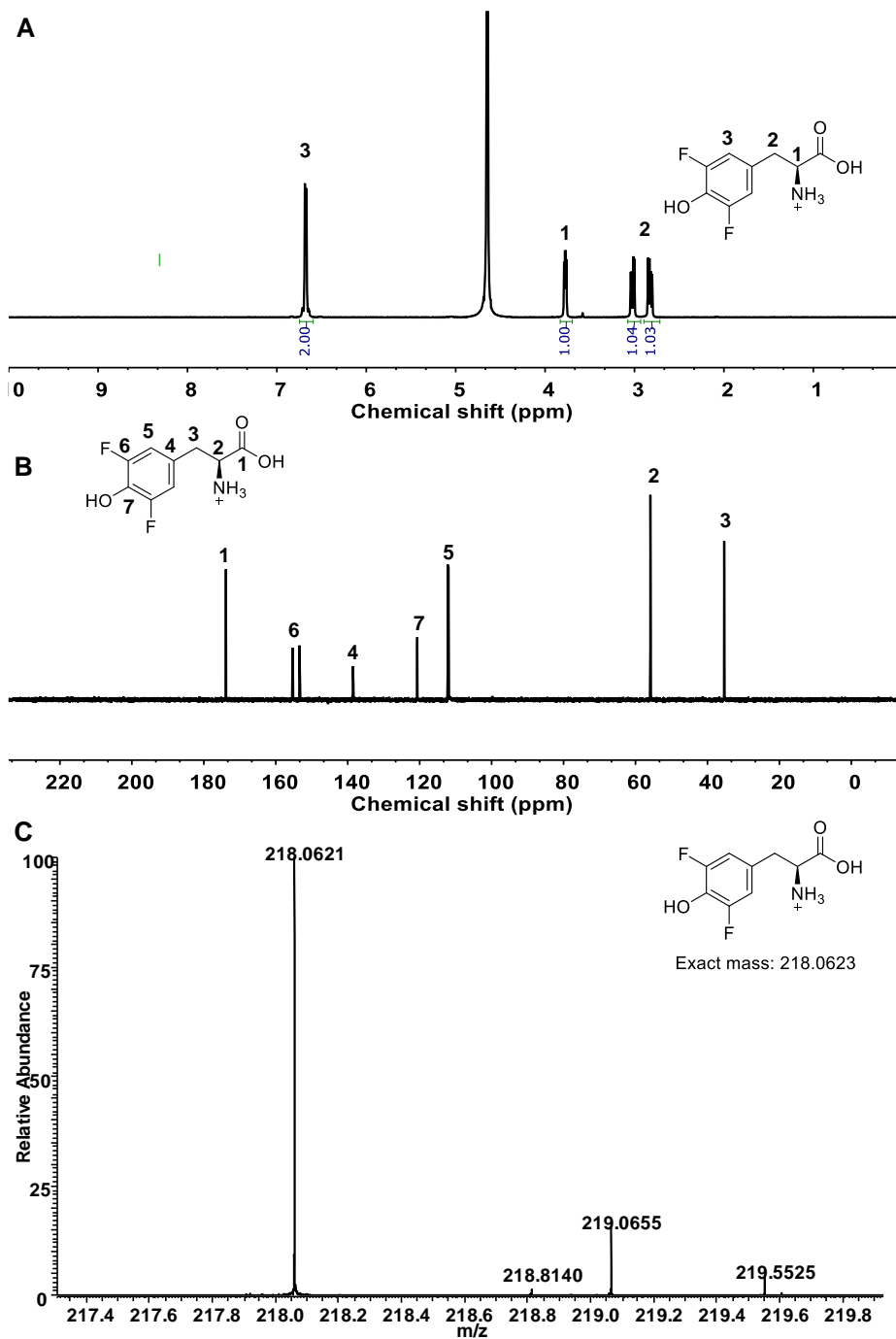


Figure S16 Characterization of 3,5-difluoro tyrosine.

(A) $^1\text{H-NMR}$ spectrum of 3,5-difluoro tyrosine. (500 MHz, D_2O): δ 6.68 (d, $J = 7.5$ Hz, 1H), 3.77 (dd, $J = 8.2, 4.9$ Hz, 1H), 3.02 (dd, $J = 14.8, 4.9$ Hz, 1H), 2.83 (dd, $J = 14.8, 8.2$ Hz, 1H). (B) $^{13}\text{C-NMR}$ spectrum of 3,5-difluoro tyrosine. (500 MHz, D_2O): δ 35.34, 55.87, 112.17, 120.68, 138.55, 153.43, 155.33, 173.85. (C) MS spectrum of 3,5-difluoro tyrosine. Calculated m/z ratio for 3,5-difluoro tyrosine ($[\text{M}+\text{H}]^+$ form, positive mode) was 218.0623 and found at 218.0621.

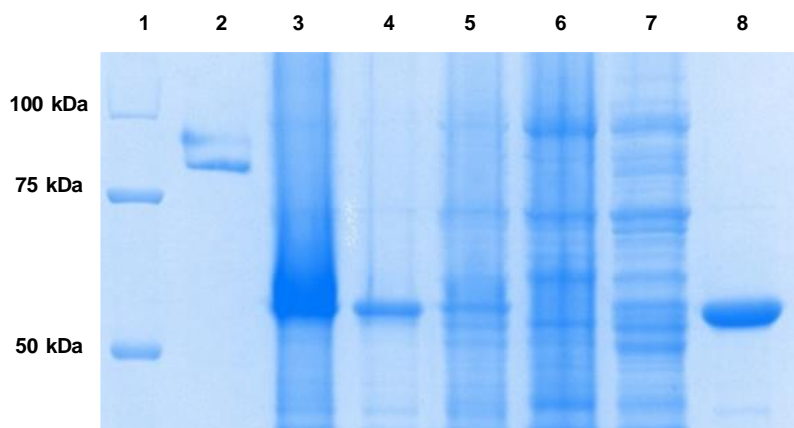


Figure S17. SDS-PAGE analysis of EanB_{Y353F2T_{YR}} purification.

Lane 1: protein marker lane 2: in-house protein standard; lane 3: cell lysate; lane 4: cell pellet; 5: supernatant; lane 6: flow-through fraction; lane 7: wash fraction; lane 8: concentrated elution.

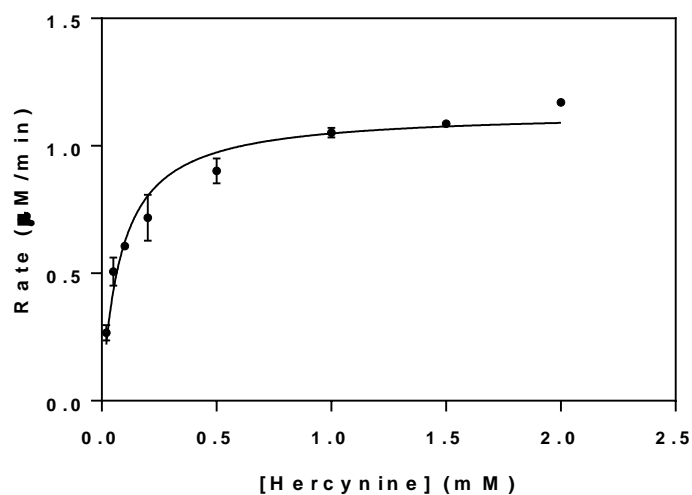


Figure S18. Hercynine concentration dependence of EanB_{Y353F2Tyr} mutant using K₂S_x as substrate.

The kinetic parameters of EanB_{Y353F2Tyr} variant are: k_{cat} of $0.42 \pm 0.01 \text{ min}^{-1}$, K_m of $82.8 \pm 9.1 \text{ } \mu\text{M}$ for hercynine. A 1-ml reaction mixture contained $2.7 \text{ } \mu\text{M}$ EanB_{Y353F2Tyr}, 400 nM ergothione (1000 equivalent of EanB activity), variable concentrations of hercynine (0.02 to 2 mM), 0.1 mM K₂S_x (using the dominant species, K₂S₄, for calculating concentration) in 50 mM KPi buffer, pH 8.0. The absorbance at 311 nm is used to monitor the reaction rate of EanB_{Y353F2Tyr}.

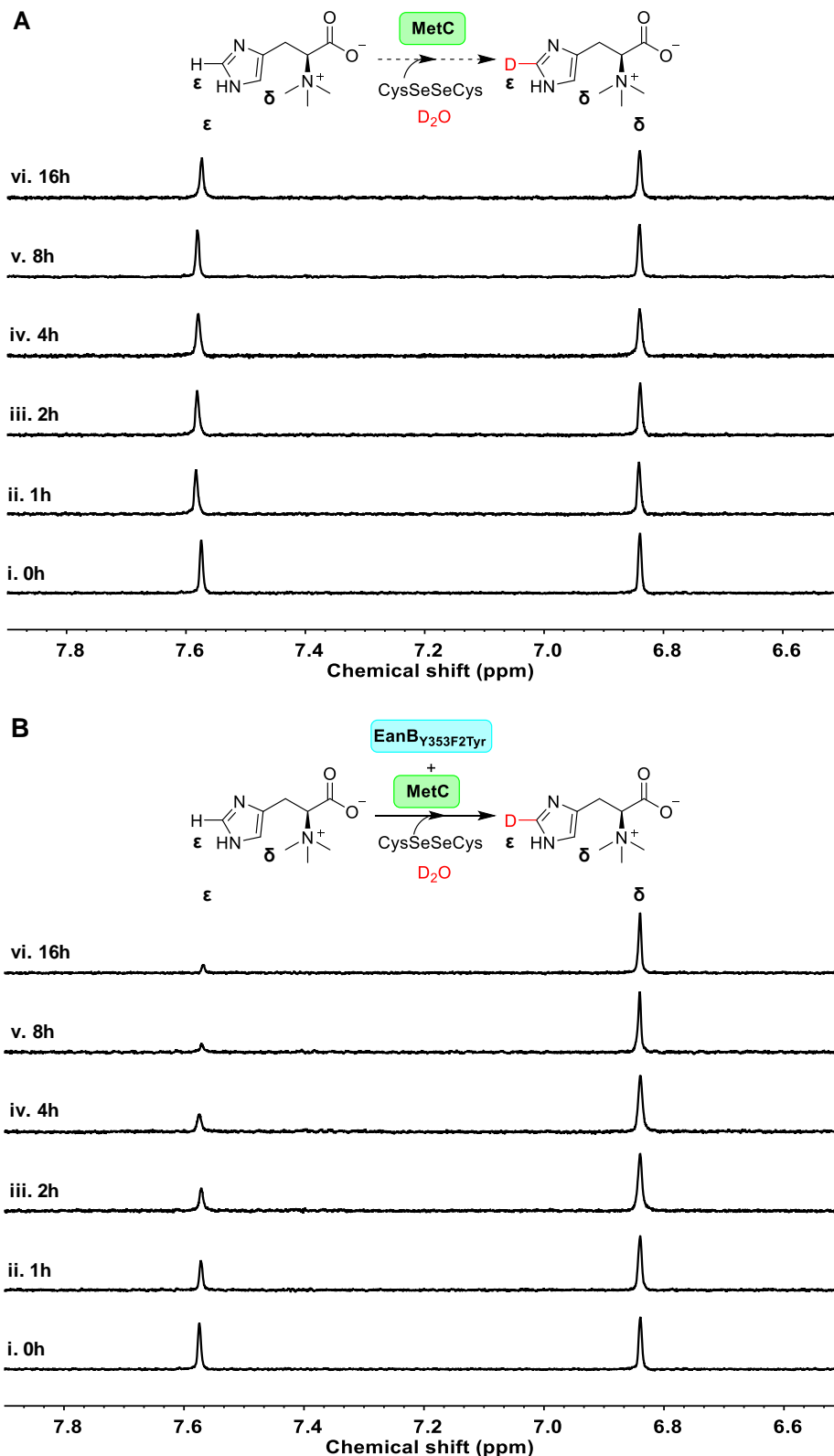


Figure S19 $^1\text{H-NMR}$ analysis of hercynine deuterium exchange experiment in EanB_{Y353F2Tyr}-MetC coupled reaction using selenocystine as substrate.

(A) Reaction mixture (2 ml) with 3mM hercynine, selenocystine saturated solution (6.7 mg powder added), 0.5 μM MetC without EanB_{Y353F2Tyr} in KPi D₂O buffer, pH 8.22 (B) Reaction mixture (2 ml) with 3mM hercynine, selenocystine saturated solution (6.7 mg powder added), 0.5 μM MetC and 12.5 μM EanB_{Y353F2Tyr} in KPi D₂O buffer, pH 8.22.

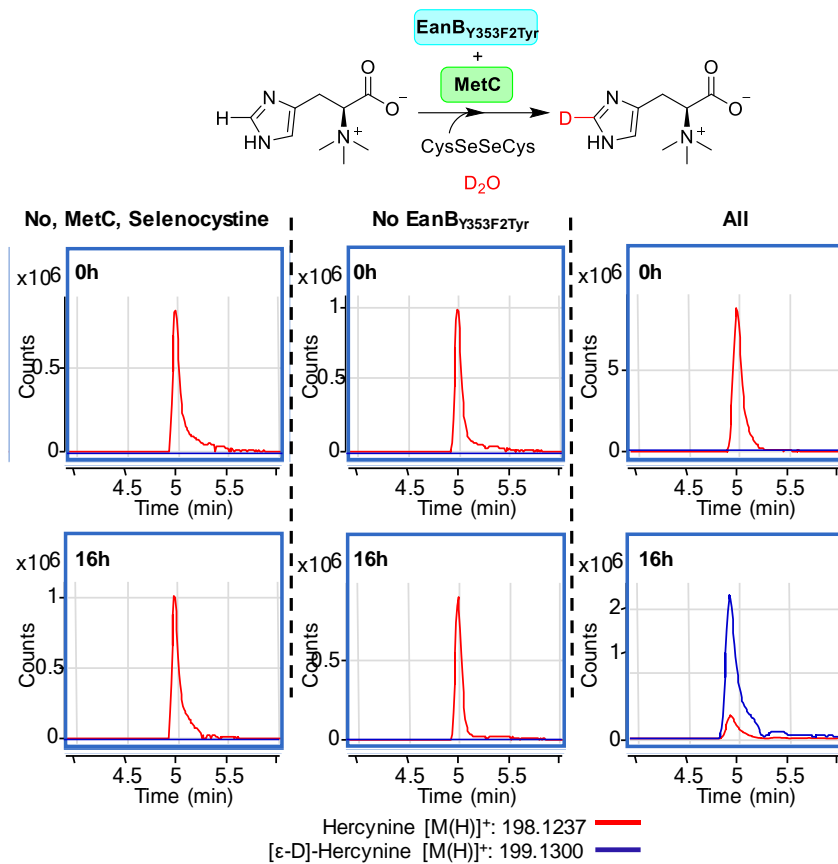


Figure S20. The extracted ion chromatograph of [ε-D]-hercynine and [ε-H] hercynine in the EanBY_{353F2Tyr} MetC coupled deuterium experiments.

The reaction mixture at 0 hour and 16 hours were withdrawn and quantified by LC-MS analysis. The 2-ml reaction mixture with all materials consists of 12.5 μM EanBY_{353F2Tyr}, 0.5 μM MetC, selenocystine saturated solution (6.7 mg powder added), 3 mM hercynine in 50 mM KPi D₂O buffer with pD of 8.22. The percentage of [ε-D]-hercynine is quantified based on the peak area between [ε-D]-hercynine (m/z: 199.1300) and hercynine (m/z: 198.1237) from the extracted ion chromatograph.

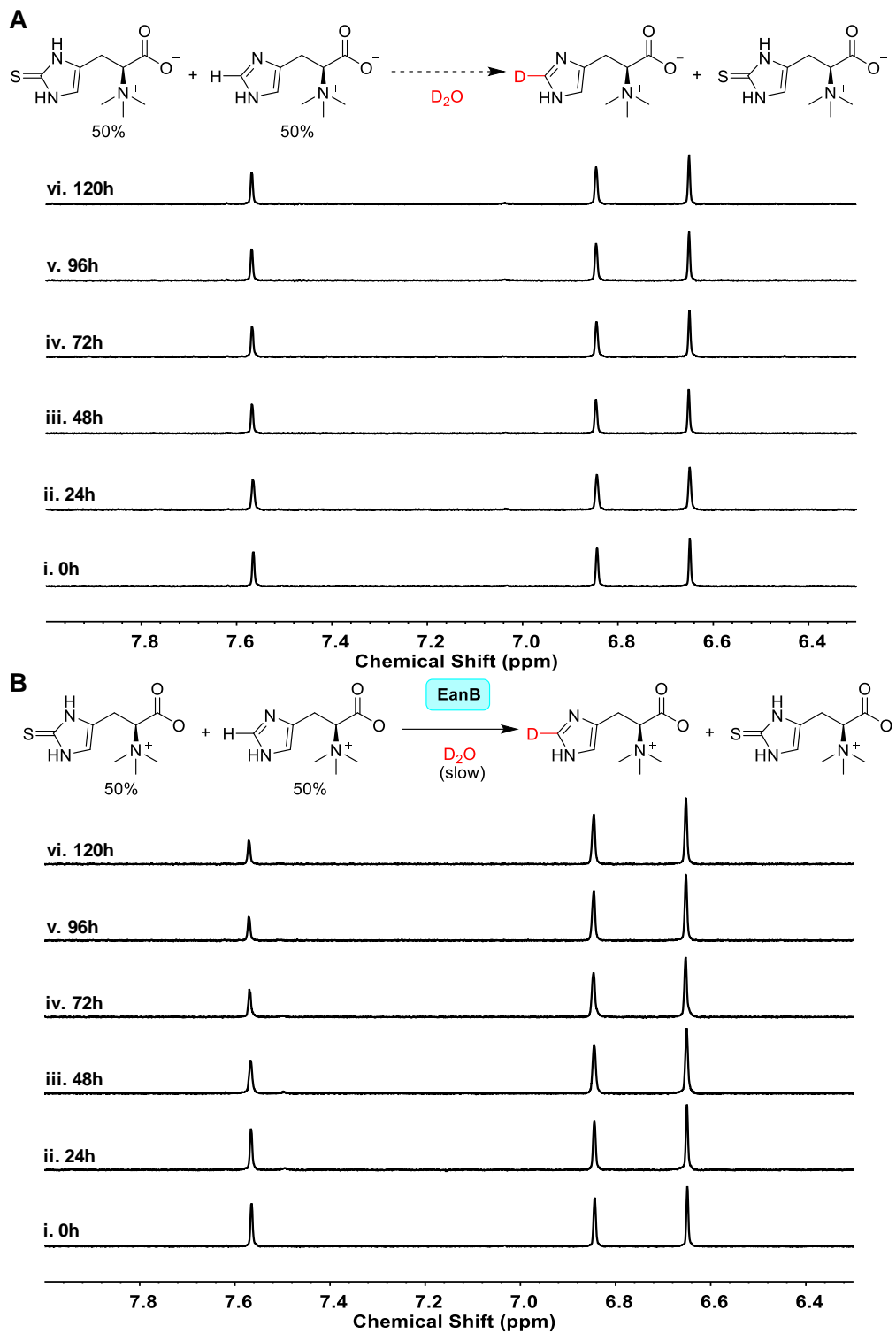


Figure S21. Deuterium exchange experiment using EanB_{WT} with equimolar hercynine and ergothioneine.

(A) Reaction mixture with 3 mM hercynine, 3 mM ergothioneine, in the absence of EanB_{WT} in KPi D₂O buffer, pD 8.22 (B) Reaction mixture with 3 mM hercynine, 3 mM ergothioneine and 50 μ M EanB_{WT} in KPi D₂O buffer, pD 8.22. The conversion of hercynine to [ϵ -²H]-hercynine is 40% after 4 days based on MS quantification.

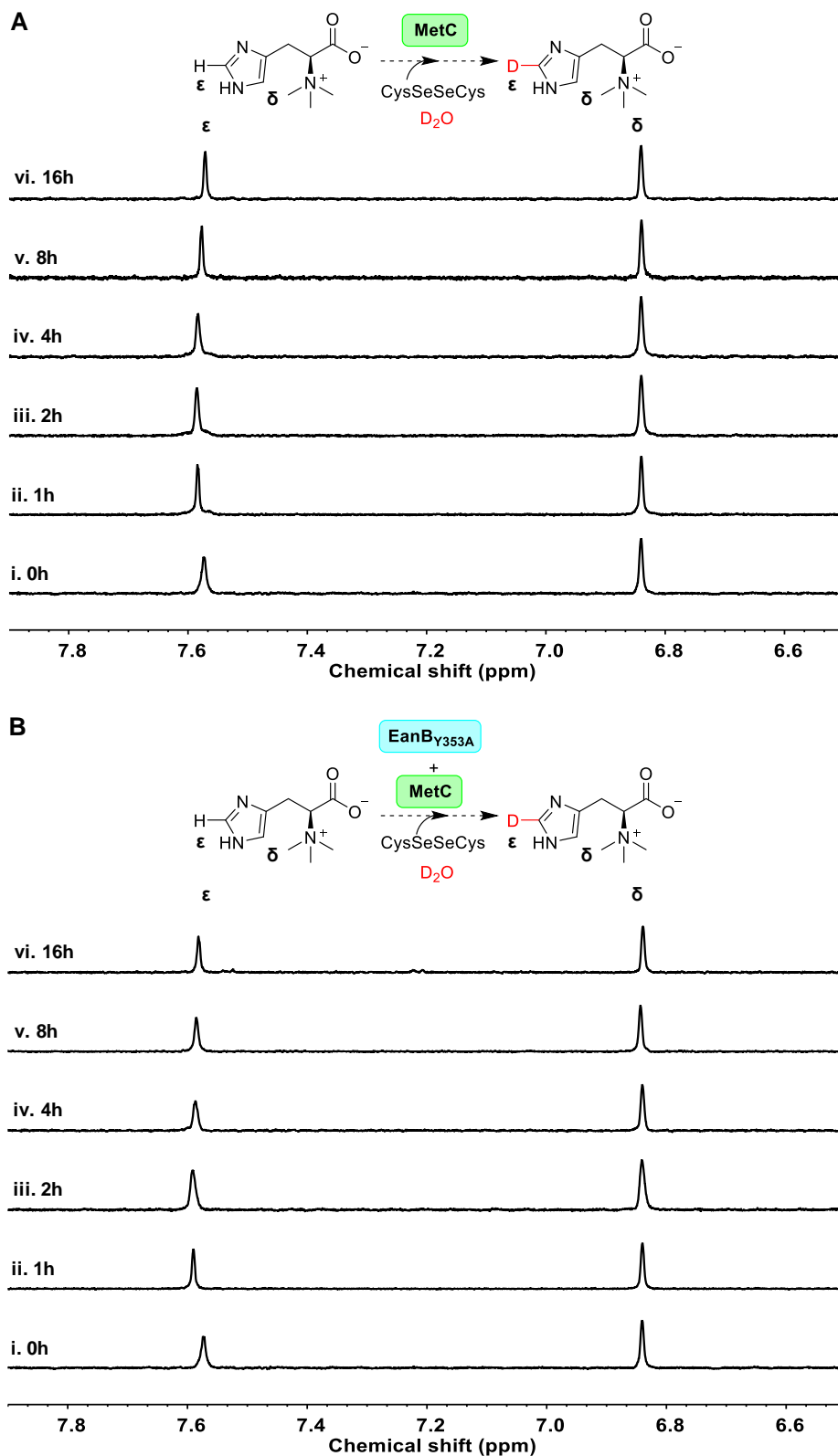


Figure S22. Hercynine deuterium exchange experiment in EanBY353A-MetC coupled reaction using selenocystine as substrate.

(A) Reaction mixture (2 ml) with 3mM hercynine, selenocystine saturated solution (6.7 mg powder added), 0.5 μ M MetC in the absence of EanBY353A in KPi D_2O buffer, pD 8.22 (B) Reaction mixture (2 ml) with 3mM hercynine, selenocystine saturated solution (6.7 mg powder added), 0.5 μ M MetC and 50 μ M EanBY353A in KPi D_2O buffer, pD 8.22.

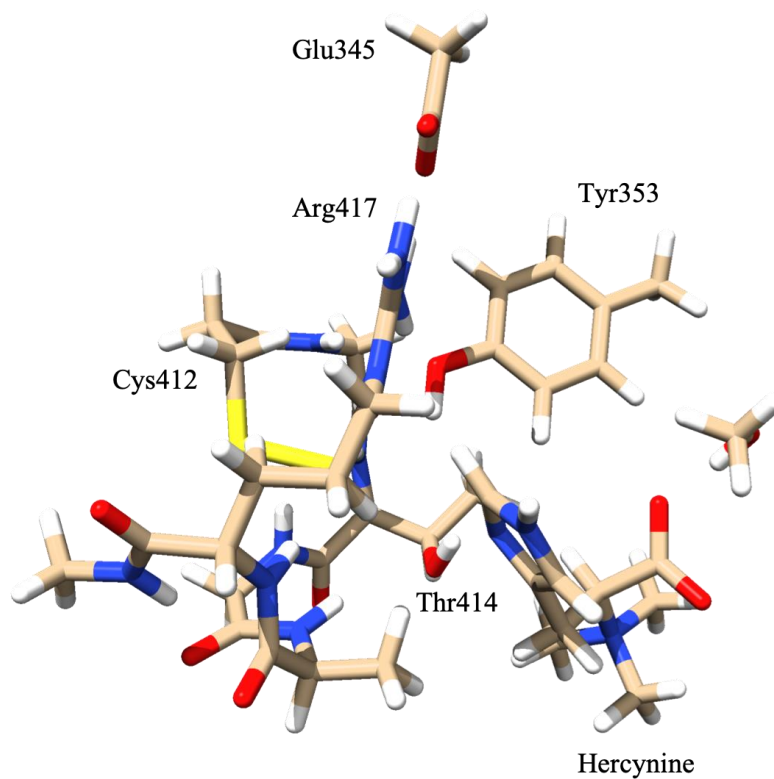


Figure S23. The QM cluster model used in the calculation.

There are 136 atoms in total for both EanB persulfide and perselenide, including atoms from Glu345, Tyr353, Tyr375, Tyr411, Cys412, Gly413, Thr414, Gly415, Trp416, Arg417 and Gly418.

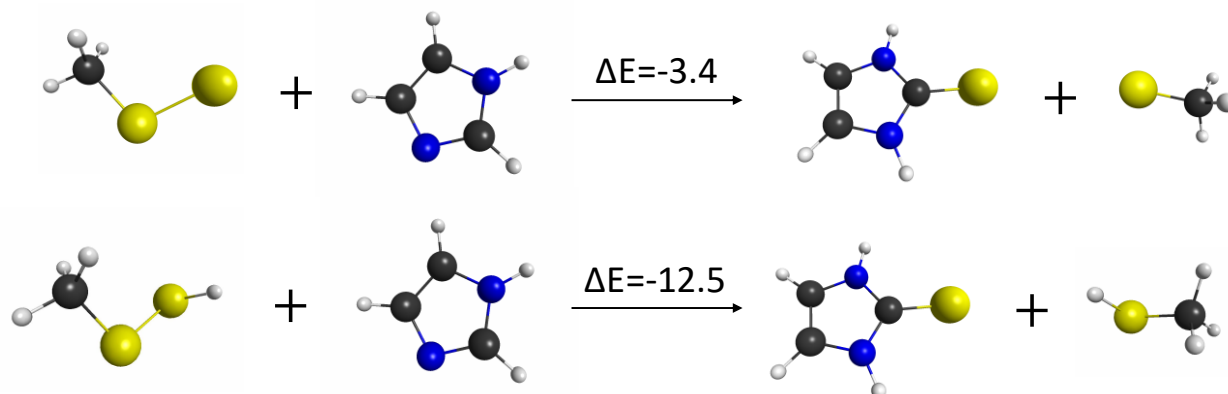


Figure S24. The reaction of persulfide with imidazole.

Energies were calculated at B3LYP-D3/6-31+G(d,p) level of theory with CPCM solvation model and a dielectric constant of 20.0. The unit for energies is kcal/mol.

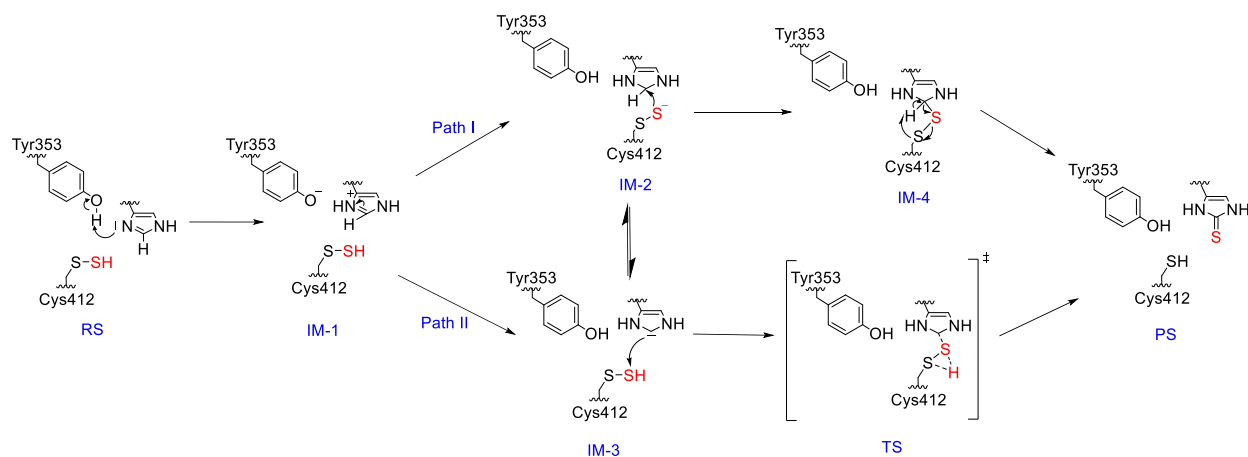


Figure S25. Proposed catalytic mechanisms for EanB with neutral persulfide.

The proposed scheme is based on results from small molecule model calculations at CPCM/B3LYP-D3/6-31+G(d,p) level of theory. **Path I:** a tetrahedral intermediate is formed after deprotonated Tyr353 accepting the proton from neutral persulfide; **Path II:** a carbene intermediate is formed after deprotonated Tyr353 accepting the proton from imidazole C-H. IM-3 and IM-4 are able to convert to each other, though small molecule calculations suggested that IM-3 may be more stable.

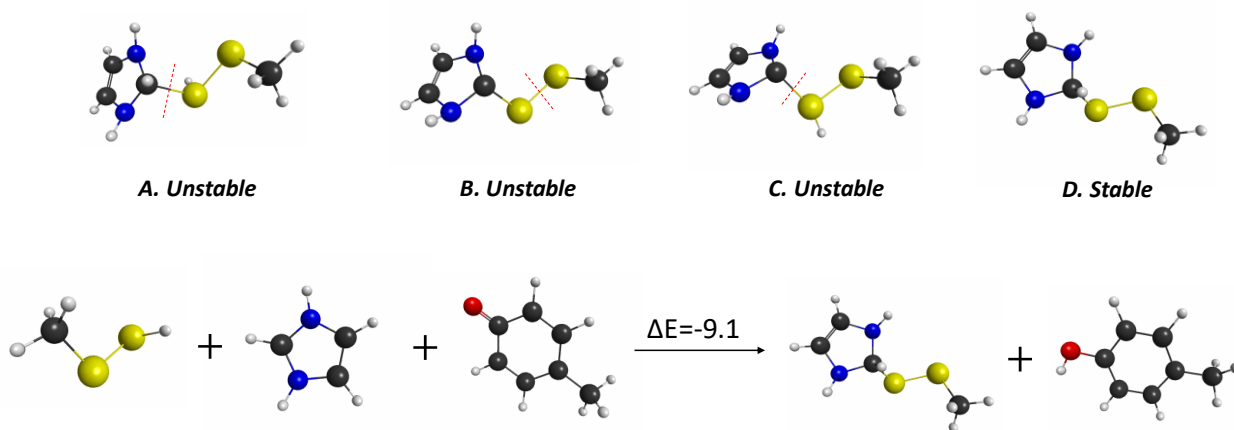


Figure S26. Possible intermediates with neutral persulfide.

Four tetrahedral/pyramidal intermediates were examined: (A). Both C and S atoms have a proton; (B). No protons on either C atom or S atom; (C). The connected S atom is protonated; (D). No proton on S atom and imidazole C atom keeps its proton; (E). The reaction for formation of the stable tetrahedral intermediate with neutral persulfide. Calculations were performed at B3LYP-D3/6-31+G(d,p) level of theory with CPCM solvation model and a dielectric constant of 20.0. The energy is in the unit of kcal/mol.

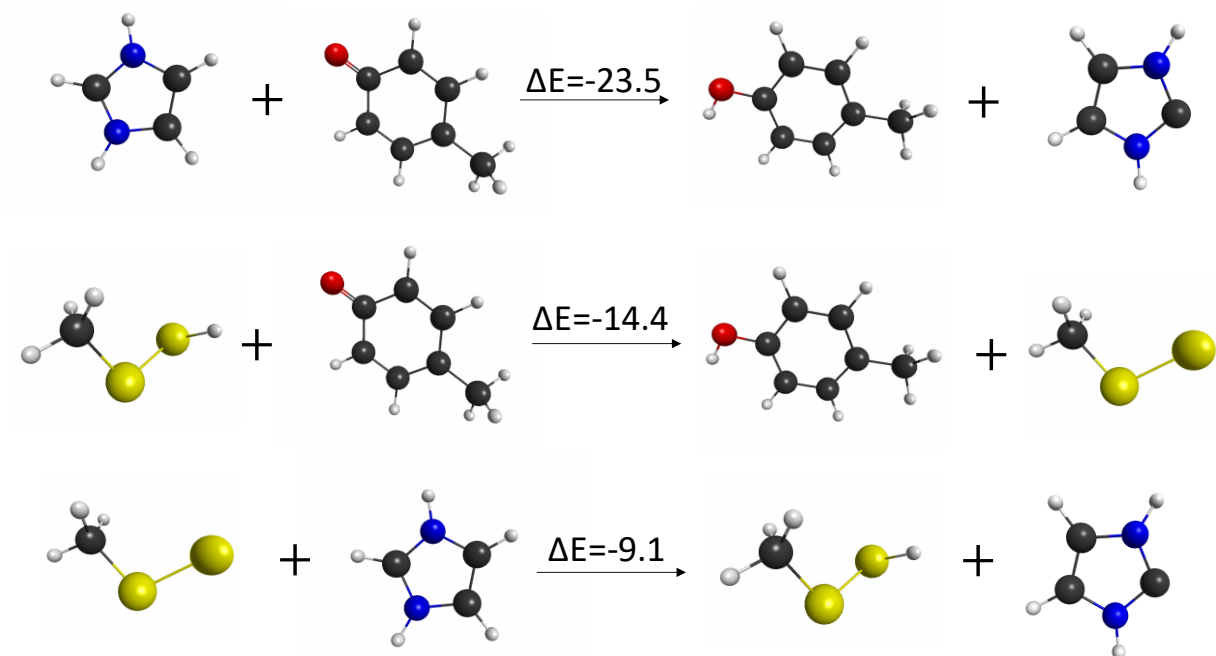


Figure S27. The possible proton transfer reactions involved in the EanB catalysis.

Calculations were performed at B3LYP-D3/6-31+G(d,p) level of theory with CPCM solvation model and a dielectric constant of 20.0. The energies are in the unit of kcal/mol.

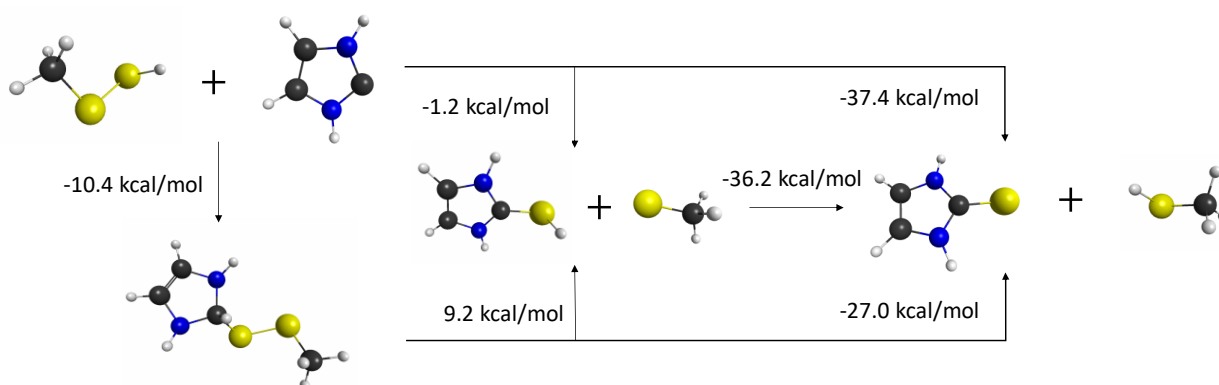


Figure S28. The possible pathways for the final step of EanB with neutral persulfide.

Calculations were performed at B3LYP-D3/6-31+G(d,p) level of theory with CPCM solvation model and a dielectric constant of 20.0.

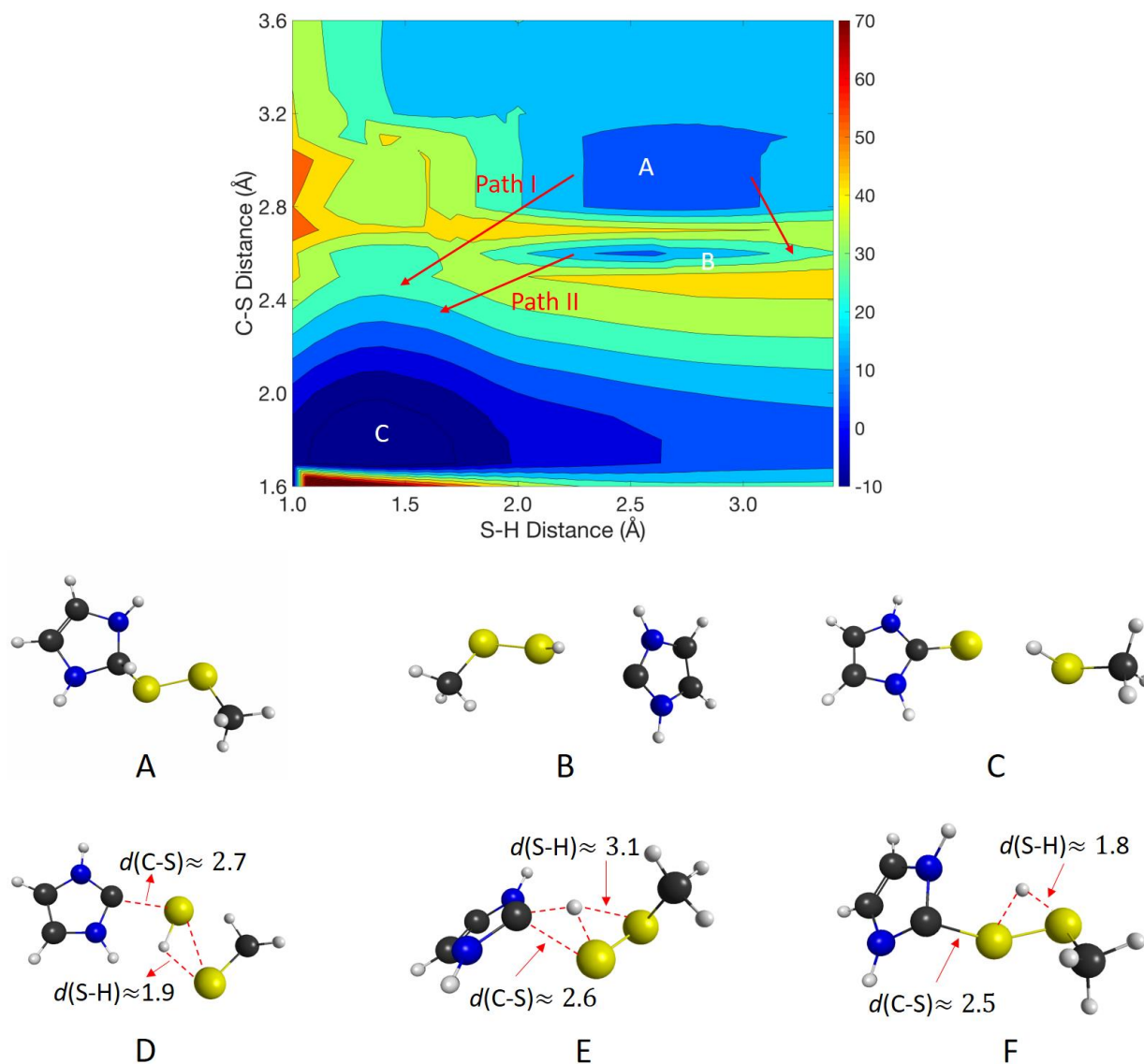


Figure S29. The potential energy surface at DFTB3/3OB level of theory for the formation of C-S bond through either a tetrahedral intermediate or carbene intermediate.

(A). The tetrahedral intermediate. (B). The carbene intermediate. (C). The final product. (D). The approximate transition state for conversion of tetrahedral intermediate (A) to the final product (C). (E). The approximate transition state for conversion of tetrahedral intermediate (A) to the carbene intermediate (B). (F). The approximate transition state for conversion of carbene intermediate (B) to the final product (C). **Path I:** tetrahedral intermediate (A) directly converts to the product (C) through a concerted pathway. **Path II:** tetrahedral intermediate converts to a carbene intermediate (B) first before the formation of final product. The energy barrier for Path I (about 45 kcal/mol) is higher than that of Path II (about 40 kcal/mol). Note: In the figure, the C-S distance refers to the distance between imidazole carbon atom and terminal persulfide sulfur atom; the S-H distance refers to the distance between the non-terminal sulfur atom of persulfide and the transferring proton. The distance is in the unit of Å. The unit for energies is kcal/mol.

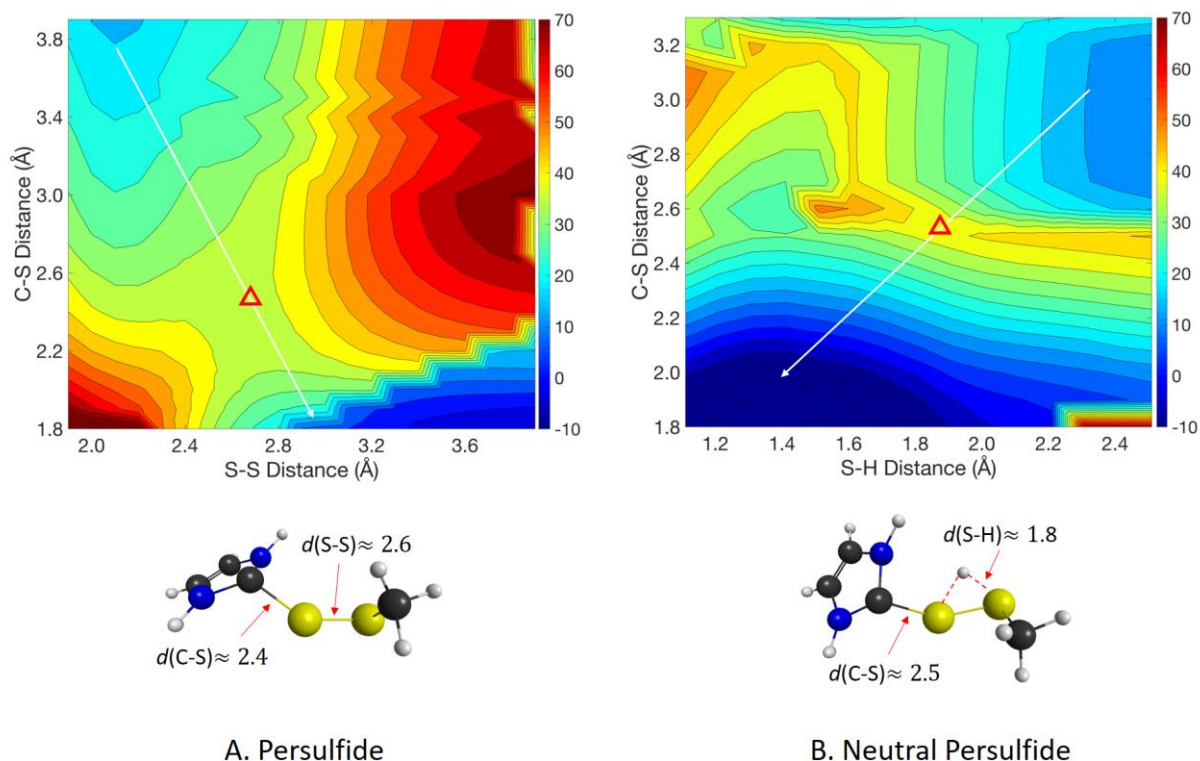


Figure S30. The potential energy surface for the product formation involving the carbene intermediate of persulfide (A) and neutral persulfide (B) at DFTB3/3OB level of theory.

The transition states for persulfide (Cys-S-S) and neutral persulfide (Cys-S-S-H) are similar in C-S and S-S distances, though neutral persulfide has a concerted transition state, in which a proton transfer reaction occurs synchronously with C-S bond formation reaction. As a result, the energy barrier for neutral persulfide is slightly higher than that of negatively charged persulfide. Note: The C-S distance refers to the distance between imidazole carbon atom and terminal persulfide sulfur atom; the S-H distance refers to the distance between the non-terminal sulfur atom of persulfide and the transferring proton. The units are Å and kcal/mol, for distance and energies, respectively.

Reference

- (1) Song, H.; Leninger, M.; Lee, N.; Liu, P., Regioselectivity of the oxidative C–S bond formation in ergothioneine and ovolthiol biosyntheses. *Org. Lett.* **2013**, *15*, 4854-4857.
- (2) Cheng, R.; Wu, L.; Lai, R.; Peng, C.; Naowarajna, N.; Hu, W.; Li, X.; Whelan, S. A.; Lee, N.; Lopez, J.; Zhao, C.; Yong, Y.; Xue, J.; Jiang, X.; Grinstaff, M. W.; Deng, Z.; Chen, J.; Cui, Q.; Zhou, J.; Liu, P., Single-Step Replacement of an Unreactive C–H Bond by a C–S Bond Using Polysulfide as the Direct Sulfur Source in the Anaerobic Ergothioneine Biosynthesis. *ACS Catal.* **2020**, 8981-8994.
- (3) Song, H.; Hu, W.; Naowarajna, N.; Her, A. S.; Wang, S.; Desai, R.; Qin, L.; Chen, X.; Liu, P., Mechanistic studies of a novel C-S lyase in ergothioneine biosynthesis: the involvement of a sulfenic acid intermediate. *Sci. Rep.* **2015**, *5*, 11870.
- (4) Seyedsayamdost, M. R.; Yee, C. S.; Stubbe, J., Site-specific incorporation of fluorotyrosines into the R2 subunit of E. coli ribonucleotide reductase by expressed protein ligation. *Nat. Protoc.* **2007**, *2*, 1225-1235.